

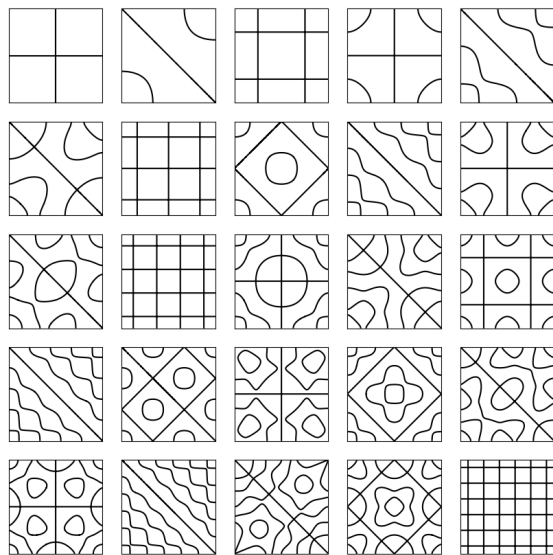
Chladni Patterns on Square and Circular Plates

Physics 4C Project

Dong D. Le and Andrew Cardona

Professor Karen Schnurbusch

June 2024



Abstract

In this study, we investigate the formation of Chladni patterns on a vibrating circular plate and examine the underlying wave dynamics. Despite our efforts, we were unable to demonstrate the constancy of wave speed across varying frequencies. Nevertheless, our experiments successfully verified Chladni's law, which relates the frequency of vibration to the number of nodal lines formed on the plate. Additionally, we uncovered a significant finding: within the framework of elastic theory, wave speed exhibits frequency dependence. This observation stands in stark contrast to the predictions of the classical wave equation model, which assumes constant wave speed regardless of frequency. Our results suggest a need for a revised understanding of wave propagation in elastic media, highlighting the limitations of traditional wave theory in explaining the complex behavior of Chladni patterns. Our findings have further introduced more questions regarding this field of study and introduced a new type of wave speed dependence that was never before thought of, thanks to our clouded knowledge around classical wave mechanics and dynamics.

Dedication

This project is dedicated to Professor Schnurbusch.
Thank you for two amazing semesters of physics.

Contents

List of Figures	5
List of Tables	6
1 Introduction and Hypothesis	7
2 The Wave Equation Model	9
2.1 The General Model of the Free Plate	9
2.2 The Square Plate	9
2.3 The Circular Plate	16
3 Designing the Plotting Algorithm	25
3.1 The Square Plate	25
3.2 The Circular Plate	27
4 Experiment Procedure and Results	29
4.1 Procedure	29
4.2 Experimental and Theoretical Results for the Square Plate	31
4.2.1 Experimental Results	31
4.2.2 Theoretical Results	31
4.2.3 Analysis	37
4.3 Experimental and Theoretical Results for the Circular Plate	38
4.3.1 Experimental Results	38
4.3.2 Theoretical Results	39
4.3.3 Analysis	39
5 The Elastic Theory Model, the Biharmonic Wave Equation, and Chladni's Law	41
5.1 Theoretical Derivation	41
5.2 Data Analysis	44
6 Conclusion	46
Appendices	48
A Mathematical Preliminaries	49
A.1 Regular Sturm-Liouville Theory	49
A.2 Singular Sturm-Liouville Theory	50

B Codes in Python	51
B.1 Starting out with Python	51
B.2 Code for the Square Wave Equation Plot	51
B.3 Code for the Circular Wave Equation Plot	54
B.4 Finding Zeros of the Derivative of the Bessel Function	55
Bibliography	57

List of Figures

2.1	First five Bessel functions of the second kind, $Y_n(x)$.	18
2.2	First five modified Bessel functions of the second kind, $K_n(x)$.	20
4.1	Experimental Results for the Square Plate	31
4.2	First 72 theoretical patterns of the square plate, plotted in Python.	32
4.3	The next 72 patterns of the square plate.	33
4.4	Pattern #145 to #216.	34
4.5	Pattern #217 to #288.	35
4.6	Experimental Results of the Square Plate	37
4.7	(Somewhat) Similar Patterns	37
4.8	Experimental Results of the Circular Plate	38
4.9	First 35 theoretical patterns of the circular plate, plotted in Python.	39
4.10	Our experimental patterns, with rings	39
4.11	Similar Patterns, where $n = 0, m = 0, 1, 2, \dots, 7$	39
5.1	Patterns with Rings in Circular Plate	44

List of Tables

4.1	The modes of the first 84 sum of squares numbers	36
4.2	Wave Speed of the Square Plate	37
4.3	Wave Speed of the Circular Plate	40
5.1	f vs. $4n^2$ table	44

Chapter 1

Introduction and Hypothesis

The theory of Chladni patterns, attributed to the German physicist and musician Ernst Chladni, serves as a classical illustration of two-dimensional standing waves. In contrast to one-dimensional standing waves, where nodes denote stationary segments of the wave, the extension to two dimensions introduces nodal lines, representing regions where no motion is present. These fascinating patterns arise from the establishment of standing waves on the surface of a plate, where specific points remain motionless while others oscillate with varying amplitudes. The emergence of these patterns is governed by factors such as the frequency, material composition of the plate, and boundary conditions. The mathematical framework describing this phenomenon is articulated through the two-dimensional wave equation [1]:

$$u_{tt} = c^2 \nabla^2 u + Q(x, y, t), \quad -a \leq x, y \leq a, \quad (1.0.1)$$

where c denotes the wave speed, which depends on the material; ∇^2 is the Laplacian of a function; and $Q(x, y, t)$ is the forcing term, which represents our wave generator. Throughout this project, we will use two types of plates, one is rectangular, which uses the wave equation in the Cartesian coordinate above, while the other one is circular, where the Laplacian will be converted to polar coordinates and defined as

$$\nabla^2 := \frac{\partial^2}{\partial r^2} + \frac{1}{r} \frac{\partial}{\partial r} + \frac{1}{r^2} \frac{\partial^2}{\partial \theta^2}. \quad (1.0.2)$$

Applying appropriate boundary conditions and solving this differential equation will output a four-dimensional function $u(x, y, t)$, but by pinpointing certain time points t_0 , we will obtain the approximated pattern by graphing the contour plot of the solutions $u(x, y, t_0)$ and $u(r, \theta, t_0)$. For a free boundary square plate, the boundary-initial conditions to this equation are:

$$u_x(\pm a, y, t) = u_y(x, \pm a, t) = 0$$

and,

$$\begin{aligned} u(x, y, 0) &= f(x, y), \\ u_t(x, y, 0) &= g(x, y) \end{aligned} \quad (1.0.3)$$

Through this experiment, we will test the two-dimensional wave equation in both square and circular plates and compare it to mathematical equivalents, restricted by the boundaries listed above. We will prove that the wave speed is constant at various frequencies. The solution to the wave equation above is determined by

$$u(x, y, t) = \frac{1}{4} A_{00} + \sum_{n \geq 1} \sum_{m \geq 1} X_n(x) Y_m(y) T(t), \quad (1.0.4)$$

where $X_n(x) = A_n \cos(k_x x) + B_n \sin(k_x x)$, $Y_m(y) = C_m \cos(k_y y) + D_m \sin(k_y y)$, and $T(t) = \cos(\omega t - \gamma)$. The solution of the wave equation with the above boundary conditions will be discussed in detail in the next section ¹.

The Square Plate. Each pattern obtained from the function above corresponds to a unique combination of ordered pairs n and m , which are simply all sum of squares combinations of perfect integers that add to $16a^2f^2/c^2$, or more specifically, as shown below

$$\frac{16a^2}{c^2}f^2 = n^2 + m^2.$$

Here, a is half the length of the plate, f is the frequency, and c is the wave speed. By determining the frequency f of the wave generator and comparing it with the anticipated pattern, we can identify these pairs of n and m . Utilizing this information, we derive the wave speed using the formula

$$c = \frac{2Lf}{\sqrt{n^2 + m^2}}, \quad L = 2a. \quad (1.0.5)$$

Using this formula, we will attempt to prove that the wave speed c is constant.

The Circular Plate. Similar to the square plate, we also derived the wave speed of the circular plate to be

$$c = \frac{2\pi fa}{z_{nm}}, \quad (1.0.6)$$

where a is the radius of the plate, and z_{nm} is the m -th zero of the derivative of the n -th order Bessel function of the first kind, $J_n(x)$. Similarly to the square plate, we will attempt to prove that the wave speed c is constant.

Chladni's Law. From research carried out by Ernst Chladni himself, he discovered that for a circular plate, the following relationship seems to emerge from various frequencies of the plate:

$$f = C(n + 2m)^2 \quad (1.0.7)$$

Here, n is the number of lines going to the circle center (i.e. diameter line), and m is the number of concentric circles formed by the sand on the plate. Later in 1894, Sir. Rayleigh successfully proved in *The Theory of Sound* [2] that it was indeed the case, and he was also able to derive exactly what the constant C was, based on the previous work of Gustav Kirchhoff. In this project, we will also prove through experimentation that $f = C(n + 2m)^2$. We will also validate our work and compare the obtained constant C with its true value, based on the material property and dimension of the circular plate.

¹Pages 5-23 are purely reserved for mathematical derivations. Skip to page 24 to start the experimentation and data analysis parts of the report

Chapter 2

The Wave Equation Model

2.1 The General Model of the Free Plate

We are familiar with the one-dimensional wave equation,

$$\frac{\partial^2 u}{\partial t^2} = c^2 \frac{\partial^2 u}{\partial x^2}, \quad (2.1.1)$$

where c is the wave speed. The equation is not much different in two-dimensional. In this project, we will also have a wave generator that acts as a forcing term, therefore, the equation that describes the displacement of the plate is

$$\frac{\partial^2 u}{\partial t^2} = c^2 \left(\frac{\partial^2 u}{\partial x^2} + \frac{\partial^2 u}{\partial y^2} \right) + Q(x, y, t) \quad (2.1.2)$$

Depending on the state of the plate (clamped, simply supported, or free), we will have different sets of boundary conditions. In this project, our plate is allowed to move freely, so the boundary condition is

$$\frac{\partial u}{\partial x}(\pm a, y, t) = \frac{\partial u}{\partial y}(0, \pm a, t) = 0 \quad (2.1.3)$$

In the two subsections below, we will derive the solution for the square, and circular wave equation with free boundary conditions. For more detailed mathematical preliminaries, we recommended two excellent books *Introduction to Applied Partial Differential Equation* by John M. Davis [3] and *Applied Partial Differential Equations with Fourier Series and Boundary Value Problems* by Richard Haberman [4].

2.2 The Square Plate

The Wave Equation. Consider the wave equation

$$\frac{\partial^2 u}{\partial t^2} = c^2 \left(\frac{\partial^2 u}{\partial x^2} + \frac{\partial^2 u}{\partial y^2} \right) + Q(x, y, t), \quad \text{or} \quad u_{tt} = c^2 \nabla^2 u + Q, \quad -a \leq x, y \leq a \quad (2.2.1)$$

with boundary conditions

$$u_x(\pm a, y, t) = u_y(x, \pm a, t) = 0$$

and initial conditions

$$u(x, y, 0) = f(x, y),$$

$$u_t(x, y, 0) = g(x, y)$$

Analytic Solution. We shall solve this problem using a common technique: separation of variables. Let $u(x, y, t) = X(x)Y(y)T(t)$. We also begin by solving the homogenous case of the equation first. The PDE implies that

$$XYT'' = c^2(X''YT + XY''T) \quad (2.2.2)$$

divide both sides by c^2XYT , we obtain

$$\frac{T''}{c^2T} = \frac{X''}{X} + \frac{Y''}{Y} = -\lambda \quad (2.2.3)$$

Notice that

$$\frac{X''}{X} + \frac{Y''}{Y} = -\lambda \quad (2.2.4)$$

is constant if and only if $X''/X = -\mu$ and $Y''/Y = -\nu$, where μ and ν are themselves constants and $\lambda = \mu + \nu$. The two constants above yield two eigenvalue problems with Neumann boundary conditions:

$$X''(x) + \mu X(x) = 0, \quad X'(-a) = X'(a) = 0 \quad (2.2.5)$$

$$Y''(y) + \nu Y(y) = 0, \quad Y'(-a) = Y'(a) = 0 \quad (2.2.6)$$

We shall begin with $X''(x) + \mu X(x) = 0$, $X'(-a) = X'(a) = 0$ first.

- Case 1: $\mu = 0$. If $\mu = 0$, then the BVP (2.2.5) becomes $X''(x) = 0$, $X'(-a) = X'(a) = 0$. The general solution to this differential equation is $X(x) = Ax + B$. Taking the derivative gives $X'(x) = A$, and the boundary condition implies that $A = 0$, but B can be arbitrary. This means that $\mu_0 = 0$ must be an eigenvalue and the function

$$X_0(x) = 1, \quad (2.2.7)$$

is its corresponding eigenfunction.

- Case 2: $\mu < 0$. Let $\mu = -p^2 < 0$. The BVP (2.2.5) becomes $X''(x) - p^2 X(x) = 0$, $X'(-a) = X'(a) = 0$. The solution to this DE is $X(x) = A \cosh(px) + B \sinh(px)$. Taking the derivative gives $X'(x) = Ap \sinh(px) + Bp \cosh(px)$. Plugging in $-a$ and a gives

$$\begin{aligned} A \cosh(pa) - B \sinh(pa) &= 0 \\ A \cosh(pa) + B \sinh(pa) &= 0 \end{aligned} \quad (2.2.8)$$

Solving for A and B gives $A = B = 0$, which is a trivial solution. We don't need this, so let's throw it away. Otherwise, to make this system non-trivial, it must be true that

$$\det \begin{bmatrix} \cosh(pa) & -\sinh(pa) \\ \cosh(pa) & \sinh(pa) \end{bmatrix} = 2 \cosh(pa) \sinh(pa) = 0 \quad (2.2.9)$$

Since $\cosh(pa) > 0 \ \forall pa \in \mathbb{R}$, it must be the case that $\sinh(pa) = 0$, or $pa = 0$, or $p = 0$. This contradicts our choice of eigenvalue, therefore λ in this case cannot be an eigenvalue, and there are no eigenfunctions.

- Case 3: $\mu > 0$. Let $\mu = p^2 > 0$. The BVP (2.2.5) becomes $X''(x) + p^2 X(x) = 0$, $X'(-a) = X'(a) = 0$. The solution to this DE is $X(x) = A \cos(px) + B \sin(px)$. Taking the derivative gives $X'(x) = -Ap \sin(px) + Bp \cos(px)$, and applying the boundary condition,

$$X'(-a) = Ap \sin(pa) + Bp \cos(pa) = 0 \implies A \sin(pa) + B \cos(pa) = 0 \quad (2.2.10)$$

$$X'(a) = -Ap \sin(pa) + Bp \cos(pa) = 0 \implies A \sin(pa) - B \cos(pa) = 0 \quad (2.2.11)$$

Adding (2.2.10) and (2.2.11), we obtain $2A \sin(pa) = 0$. This implies that either $A = 0$ or $\sin(pa) = 0$. Subtracting (2.2.11) from (2.2.10) gives $2B \cos(pa) = 0$. This implies that either $B = 0$ or $\cos(pa) = 0$. To summarize, we have

$$A = 0, \text{ or } \sin(pa) = 0, \quad \text{and} \quad B = 0 \text{ or } \cos(pa) = 0. \quad (2.2.12)$$

Together, they form four cases: $A = B = 0$, $A = \cos(pL) = 0$, and $B = \sin(pL) = 0$, and the final one gives $\cos(pL) = \sin(pL) = 0$, which is not possible. The second, and third case gives

$$p_1 = \frac{n\pi}{a} \quad \text{and} \quad p_2 = \frac{(n - \frac{1}{2})\pi}{a}, \quad n = 1, 2, 3, \dots, \quad (2.2.13)$$

respectively. Therefore, there are only two non-trivial families of solutions in this case, giving the corresponding eigenvalues

$$\mu_{n,1} = \left(\frac{n\pi}{a}\right)^2, \quad \text{and} \quad \mu_{n,2} = \left(\frac{(n - \frac{1}{2})\pi}{a}\right)^2 \quad (2.2.14)$$

However, looking at the n -terms, we see that

$$\{n\}_{n=1}^{\infty} = \{1, 2, 3, 4, \dots\} \quad \text{and} \quad \left\{n - \frac{1}{2}\right\}_{n=1}^{\infty} = \left\{\frac{1}{2}, \frac{3}{2}, \frac{5}{2}, \frac{7}{2}, \dots\right\} \quad (2.2.15)$$

Therefore, we can combine two families of eigenvalues into one family, obtaining

$$\mu = \left(\frac{n\pi}{2a}\right)^2 \quad (2.2.16)$$

and the corresponding eigenfunction is

$$X_n(x) = \begin{cases} \sin\left(\frac{n\pi x}{2a}\right) & \text{if } n \text{ is odd} \\ \cos\left(\frac{n\pi x}{2a}\right) & \text{if } n \text{ is even} \end{cases}, \quad n = 1, 2, 3, \dots \quad (2.2.17)$$

We can do a bit better than this. Define

$$a_n = \frac{1 + (-1)^n}{2} = \begin{cases} 0 & \text{if } n \text{ is odd} \\ 1 & \text{if } n \text{ is even} \end{cases}, \quad \text{and} \quad \bar{a}_n = \frac{1 - (-1)^n}{2} = \begin{cases} 1 & \text{if } n \text{ is odd} \\ 0 & \text{if } n \text{ is even} \end{cases} \quad (2.2.18)$$

Now, $X_n(x)$ can be written into a single line:

$$X_n(x) = \frac{1 - (-1)^n}{2} \sin\left(\frac{n\pi x}{2a}\right) + \frac{1 + (-1)^n}{2} \cos\left(\frac{n\pi x}{2a}\right) \quad (2.2.19)$$

The X Function. Combining with the case $\mu = 0$, we now have

$$X_0(x) = 1, \quad X_n(x) = \frac{1 + (-1)^n}{2} \cos\left(\frac{n\pi x}{2a}\right) + \frac{1 - (-1)^n}{2} \sin\left(\frac{n\pi x}{2a}\right), \quad n = 1, 2, 3, \dots \quad (2.2.20)$$

The Y Function. Repeat the exact same process for $Y(y)$, and index differently, we obtain

$$Y_0(y) = 1, \quad Y_m(y) = \frac{1 + (-1)^m}{2} \cos\left(\frac{m\pi y}{2a}\right) + \frac{1 - (-1)^m}{2} \sin\left(\frac{m\pi y}{2a}\right), \quad m = 1, 2, 3, \dots \quad (2.2.21)$$

The Time Function. Recall that

$$\lambda = \mu + \nu = \left(\frac{n\pi}{2a}\right)^2 + \left(\frac{m\pi}{2a}\right)^2 > 0 \quad (2.2.22)$$

The reason why $\lambda \neq 0$ is because the eigenvalues μ and ν are obtained from $n, m = 1, 2, 3, \dots$, and therefore we only need to consider the case $\lambda > 0$. For the case $\lambda > 0$, $T_{nm}(t) = A_{nm} \cos(c\sqrt{\lambda_{nm}}t) + B_{nm} \sin(c\sqrt{\lambda_{nm}}t)$. We now have one solution of the equation:

$$u(x, y, t) = X_n(x)Y_m(y)T_{nm}(t), \quad (2.2.23)$$

where,

$$\begin{aligned} X_n(x) &= a_n \cos(\sqrt{\mu_n}x) + \bar{a}_n \sin(\sqrt{\mu_n}x) \\ Y_m(y) &= a_m \cos(\sqrt{\nu_m}y) + \bar{a}_m \sin(\sqrt{\nu_m}y) \\ T_{nm}(t) &= A_{nm} \cos(c\sqrt{\lambda_{nm}}t) + B_{nm} \sin(c\sqrt{\lambda_{nm}}t) \end{aligned} \quad (2.2.24)$$

By the principle of superposition, the linear combination of all solutions is the general solution,

$$u(x, y, t) = c_{00}X_0(x)Y_0(y) + \sum_{n=1}^{\infty} \sum_{m=1}^{\infty} c_{nm}X_n(x)Y_m(y)T_{nm}(t) \quad (2.2.25)$$

Recall that we took $X_0 = Y_0 = 1$, and for convenience, denote c_{00} as $\frac{1}{4}A_{00}$.

$$u(x, y, t) = \frac{1}{4}A_{00} + \sum_{n=1}^{\infty} \sum_{m=1}^{\infty} X_n(x)Y_m(y)T_{nm}(t). \quad (2.2.26)$$

The Coefficient. We start by noting that $\{\alpha, X_n(x)\}_{n=1}^{\infty}$ (α is any constant) and $\{X_n(x)\}_{n=1}^{\infty}$ form an orthogonal family on $-a < x < a$. Another thing to note here is that

$$a_n \bar{a}_n = \left(\frac{1 + (-1)^n}{2}\right) \left(\frac{1 - (-1)^n}{2}\right) = \frac{1 - (-1)^n + (-1)^n - (-1)^{2n}}{4} = 0 \quad (2.2.27)$$

Based on the initial condition,

$$u(x, y, 0) = \frac{1}{4}A_{00} + \sum_{n=1}^{\infty} \sum_{m=1}^{\infty} X_n(x)Y_m(y)A_{nm} = f(x, y). \quad (2.2.28)$$

Multiply both sides by $X_p(x)$ and $Y_q(y)$, and integrate,

$$\begin{aligned} \frac{1}{4}A_{00} \underbrace{\int_{-a}^a \int_{-a}^a X_p(x)Y_q(y)dx dy}_0 + \sum_{n=1}^{\infty} \sum_{m=1}^{\infty} A_{nm} \int_{-a}^a \int_{-a}^a X_n(x)X_p(x)Y_m(y)Y_q(y) dx dy \\ = \int_{-a}^a \int_{-a}^a f(x, y)X_p(x)Y_q(y) dx dy \end{aligned} \quad (2.2.29)$$

and since $\{X_n(x)\}, \{Y_m(y)\}$ form orthogonal families,

$$A_{pq} \int_{-a}^a \int_{-a}^a X_p^2(x) Y_p^2(y) dx dy = \int_{-a}^a \int_{-a}^a f(x, y) X_p(x) Y_q(y) dx dy \quad (2.2.30)$$

Now, recall that $a_n \bar{a}_n = 0$, and note that

$$\begin{aligned} \int_{-a}^a X_n^2(x) dx &= \int_{-a}^a \left(a_n \cos\left(\frac{n\pi}{2a}x\right) + \bar{a}_n \sin\left(\frac{n\pi}{2a}x\right) \right) \left(a_n \cos\left(\frac{n\pi}{2a}x\right) + \bar{a}_n \sin\left(\frac{n\pi}{2a}x\right) \right) dx \\ &= \int_{-a}^a a_n^2 \cos\left(\frac{n\pi}{2a}x\right)^2 + \bar{a}_n^2 \sin\left(\frac{n\pi}{2a}x\right)^2 dx \\ &= a_n^2 \underbrace{\int_{-a}^a \cos\left(\frac{n\pi}{2a}x\right)^2 dx}_{a} + \bar{a}_n^2 \underbrace{\int_{-a}^a \sin\left(\frac{n\pi}{2a}x\right)^2 dx}_{a} \\ &= a \underbrace{[a_n^2 + \bar{a}_n^2]}_1 \\ &= a \end{aligned} \quad (2.2.31)$$

Therefore,

$$A_{pq} \int_{-a}^a \int_{-a}^a X_p^2(x) Y_p^2(y) dx dy = A_{pq} \int_{-a}^a X_p^2(x) dx \int_{-a}^a Y_p^2(y) dy = a^2 \quad (2.2.32)$$

Since p, q are arbitrary, we can just replace it with m, n and obtain

$$A_{nm} = \frac{1}{a^2} \int_{-a}^a \int_{-a}^a f(x, y) X_n(x) Y_m(y) dx dy \quad (2.2.33)$$

For B_{nm} , take time the derivative of $u(x, y, t)$, $u_t = XYc\sqrt{\lambda_{mn}}(-A_{nm} \sin(c\sqrt{\lambda_{mn}}t) + B_{nm} \cos(c\sqrt{\lambda_{mn}}t))$ and substitute $t = 0$,

$$u_t(x, y, 0) = \sum_{n=1}^{\infty} \sum_{m=1}^{\infty} X_n(x) Y_m(y) B_{nm} c\sqrt{\lambda_{mn}} = g(x, y)$$

Repeat the same process all over again, we obtain

$$B_{nm} = \frac{1}{a^2} \int_{-a}^a \int_{-a}^a \frac{g(x, y)}{c\sqrt{\lambda_{mn}}} X_n(x) Y_m(y) dx dy \quad (2.2.34)$$

Finally, repeat again for $\frac{1}{4}A_{00}$ by multiplying $\frac{1}{4}A_{00}$ and integrate:

$$\int_{-a}^a \int_{-a}^a \left(\frac{1}{4}A_{00} \right)^2 dx dy + \sum_{n=1}^{\infty} \sum_{m=1}^{\infty} \int_{-a}^a \int_{-a}^a \frac{1}{4}A_{00} X_n(x) Y_m(y) T_{nm}(t) dx dy = \int_{-a}^a \int_{-a}^a \frac{1}{4}A_{00} f(x, y) dx dy \quad (2.2.35)$$

Since $\{\frac{1}{4}A_{00}, X_n(x)\}$ and $\{\frac{1}{4}A_{00}, Y_m(y)\}$ form two orthogonal families, the infinite series vanishes, leaving behind

$$\int_{-a}^a \int_{-a}^a \left(\frac{1}{4}A_{00} \right)^2 dx dy = \left(\frac{1}{4}A_{00} \right)^2 4a^2 = \int_{-a}^a \int_{-a}^a \frac{1}{4}A_{00} f(x, y) dx dy, \quad (2.2.36)$$

and therefore

$$A_{00} = \frac{1}{a^2} \int_{-a}^a \int_{-a}^a f(x, y) dx dy = \frac{1}{a^2} \int_{-a}^a \int_{-a}^a f(x, y) X_0(x) Y_0(y) dx dy \quad (2.2.37)$$

The Angular Frequency. Finally, let $\omega_{nm} = c\sqrt{\lambda_{nm}}$. It follows that

$$\omega_{nm} = ck = c\sqrt{k_x^2 + k_y^2} = c\sqrt{\left(\frac{n\pi}{2a}\right)^2 + \left(\frac{m\pi}{2a}\right)^2} = \frac{\pi}{2a}c\sqrt{n^2 + m^2} \quad (2.2.38)$$

Since $\omega = 2\pi f$,

$$2\pi f = \frac{\pi}{2a}c\sqrt{n^2 + m^2} \implies f = \frac{c}{4a}\sqrt{n^2 + m^2} \implies \frac{16a^2}{c^2}f^2 = n^2 + m^2 \quad (2.2.39)$$

Complementary Solution. Substitute $a = L/2$, the final homogeneous solution to the free-edge wave equation is given by

$$u(x, y, t) = \frac{1}{4}A_{00} + \sum_{n=1}^{\infty} \sum_{m=1}^{\infty} X_n(x)Y_m(y) [A_{nm} \cos(\omega_{nm}t) + B_{nm} \sin(\omega_{nm}t)], \quad (2.2.40)$$

where

$$X_n(x) = a_n \cos\left(\frac{n\pi x}{L}\right) + \bar{a}_n \sin\left(\frac{n\pi x}{L}\right) \quad (2.2.41)$$

$$Y_m(y) = a_m \cos\left(\frac{m\pi y}{L}\right) + \bar{a}_m \sin\left(\frac{m\pi y}{L}\right) \quad (2.2.42)$$

$$\omega_{nm} = \frac{\pi}{L}c\sqrt{n^2 + m^2} \quad (2.2.43)$$

and,

$$A_{nm} = \frac{4}{L^2} \int_{-L/2}^{L/2} \int_{-L/2}^{L/2} f(x, y) X_n(x) Y_m(y) dx dy, \quad n, m = 0, 1, 2, \dots \quad (2.2.44)$$

$$B_{nm} = \frac{4}{L^2} \int_{-L/2}^{L/2} \int_{-L/2}^{L/2} \frac{g(x, y)}{\omega_{nm}} X_n(x) Y_m(y) dx dy, \quad n, m = 1, 2, 3, \dots \quad (2.2.45)$$

Particular Solution. Suppose the general solution can be written as

$$u(x, y, t) = C + \sum_{m,n} W_{nm}(t) \phi_{nm}(x, y), \quad (2.2.46)$$

where

$$\phi_{nm}(x, y) = X(x)Y(y) = \left(a_n \cos\left(\frac{n\pi x}{L}\right) + \bar{a}_n \sin\left(\frac{n\pi x}{L}\right)\right) \left(a_m \cos\left(\frac{m\pi y}{L}\right) + \bar{a}_m \sin\left(\frac{m\pi y}{L}\right)\right)$$

Differentiating u with respect to time, we obtain

$$\frac{\partial^2 u}{\partial t^2} = \sum_{m,n} \frac{d^2 W_{nm}}{dt^2} \phi_{nm}(x, y) \quad (2.2.47)$$

With respect to x and y :

$$\nabla^2 u = \sum_{m,n} W_{nm}(t) \nabla^2 \phi_{nm}(x, y) \quad (2.2.48)$$

Since $\nabla^2 \phi_{nm} = X''Y + XY'' = -\lambda_{nm}\phi_{nm} = -\lambda_{nm}XY$,

$$\frac{\partial^2 u}{\partial t^2} - c^2 \nabla^2 u = Q(x, y, t) \implies \sum_{m,n} \left(\frac{d^2 W_{nm}}{dt^2} + c^2 \lambda_{nm} W_{nm} \right) \phi_{nm} = Q(x, y, t) \quad (2.2.49)$$

Since we know that $Q(x, y, t) \in L_1^2[-a, a]$, therefore if we expand F in terms of the eigenfunctions $\phi_i(x, y)$, then

$$Q(x, y, t) = \sum_{m,n \geq 1} q_{nm}(t) \phi_{nm}(x, y).$$

Based on Sturm-Liouville theory, the coefficients q_i are determined by

$$q_{nm}(t) = \frac{\iint_{\Omega} Q(x, y, t) \phi_{nm}(x, y) dx dy}{\iint_{\Omega} \phi_{nm}^2(x, y) dx dy} \quad (2.2.50)$$

where $\Omega = [-a, a] \times [-a, a]$. Equating two equations gives

$$\frac{d^2 W_{nm}}{dt^2} + c^2 \lambda_{mn} W_{nm} = q_{nm}(t), \quad i = 1, 2, 3, \dots$$

By variation of parameters,

$$\begin{aligned} y_p &= -\cos(\omega t) \int_0^t \frac{\sin(\omega\tau) q_{nm}(\tau)}{\omega} d\tau + \sin(\omega t) \int_0^t \frac{\cos(\omega\tau) q_{nm}(\tau)}{\omega} d\tau \\ &= \int_0^t q_{nm}(\tau) \frac{-\cos(\omega t) \sin(\omega\tau) + \sin(\omega t) \cos(\omega\tau)}{\omega} d\tau \\ &= \int_0^t q_{nm}(\tau) \frac{\sin(\omega t - \omega\tau)}{\omega} d\tau \end{aligned} \quad (2.2.51)$$

Therefore,

$$W_{nm}(t) = A_{nm} \cos(\omega t) + B_{nm} \sin(\omega t) + \int_0^t q_{nm}(\tau) \frac{\sin(\omega(t - \tau))}{\omega} d\tau \quad (2.2.52)$$

The q function. For our wave generator, since it is periodic, therefore

$$Q(x, y, t) = Q_0(x, y) \cos(\omega_0 t), \quad (2.2.53)$$

where

$$Q_0(x, y) = \begin{cases} \alpha, & \text{if } x^2 + y^2 \leq r^2 \\ 0, & \text{otherwise} \end{cases}. \quad (2.2.54)$$

Also, recall what we did up there that

$$\iint_{\Omega} \phi_{nm}^2(x, y) dA = \int_{-a}^a X_n^2(x, y) dx \int_{-a}^a Y_m^2(x, y) dy = a \cdot a = a^2 = \frac{L^2}{4}. \quad (2.2.55)$$

Therefore,

$$q_{nm}(t) = \frac{4\alpha}{L^2} \cos(\omega_0 t) \iint_{U(r)} X_n(x) Y_m(y) dx dy, \quad U(r) = \{(x, y) \in \mathbb{R}^2 \mid x^2 + y^2 \leq r^2\} \subset \Omega \quad (2.2.56)$$

Final Solution. The final solution to the forced wave equation is

$$u(x, y, t) = \frac{1}{4}A_{00} + \sum_{n=1}^{\infty} \sum_{m=1}^{\infty} X_n(x)Y_m(y)W_{nm}(t), \quad (2.2.57)$$

where

$$X_n(x) = a_n \cos\left(\frac{n\pi x}{L}\right) + \bar{a}_n \sin\left(\frac{n\pi x}{L}\right) \quad (2.2.58)$$

$$Y_m(y) = a_m \cos\left(\frac{m\pi y}{L}\right) + \bar{a}_m \sin\left(\frac{m\pi y}{L}\right) \quad (2.2.59)$$

$$W_{nm}(t) = A_{nm} \cos(\omega t) + B_{nm} \sin(\omega t) + \int_0^t q_{nm}(\tau) \frac{\sin(\omega t - \omega\tau)}{\omega} d\tau \quad (2.2.60)$$

$$\omega = \frac{\pi}{L} c \sqrt{n^2 + m^2} \quad (2.2.61)$$

and,

$$A_{nm} = \frac{4}{L^2} \int_{-L/2}^{L/2} \int_{-L/2}^{L/2} f(x, y) X_n(x) Y_m(y) dx dy, \quad n, m = 0, 1, 2, \dots \quad (2.2.62)$$

$$B_{nm} = \frac{4}{L^2} \int_{-L/2}^{L/2} \int_{-L/2}^{L/2} \frac{g(x, y)}{\omega} X_n(x) Y_m(y) dx dy, \quad n, m = 1, 2, 3, \dots \quad (2.2.63)$$

2.3 The Circular Plate

The Polar Wave Equation. Consider the wave equation

$$\frac{\partial^2 u}{\partial t^2} = c^2 \left(\frac{\partial^2 u}{\partial r^2} + \frac{1}{r} \frac{\partial u}{\partial r} + \frac{1}{r^2} \frac{\partial^2 u}{\partial \theta^2} \right) + Q(r, \theta, t) \quad (2.3.1)$$

Written in compact form with full boundary conditions:

$$\begin{cases} u_{tt} = c^2 \left(u_{rr} + \frac{1}{r} u_r + \frac{1}{r^2} u_{\theta\theta} \right) + Q, & 0 < r < a, 0 < \theta < 2\pi \\ u_r(a, \theta, t) = 0 \\ u(r, \theta, 0) = f(r, \theta) \\ u_t(r, \theta, 0) = g(r, \theta) \end{cases} \quad (2.3.2)$$

Solution. Again, suppose $u = R(r)\Theta(\theta)T(t)$

$$R\Theta T'' = c^2 \left(R''\Theta T + \frac{1}{r} R'\Theta T + \frac{1}{r^2} R\Theta'' T \right) \quad (2.3.3)$$

Divide both sides by $c^2 R\Theta T$, we obtain

$$\frac{T''}{c^2 T} = \frac{R''}{R} + \frac{1}{r} \frac{R'}{R} + \frac{1}{r^2} \frac{\Theta''}{\Theta} = -\lambda \quad (2.3.4)$$

Again, the summation in the middle equation implies that each of them must also be constant, and therefore

$$\frac{R''}{R} + \frac{1}{r} \frac{R'}{R} + \lambda = \frac{1}{r^2} \nu, \quad \frac{1}{r^2} \frac{\Theta''}{\Theta} = -\frac{1}{r^2} \nu \quad (2.3.5)$$

This gives three eigenvalue problems:

$$T'' + \lambda c^2 T = 0 \quad (2.3.6)$$

$$\Theta'' + \nu \Theta = 0, \quad \Theta(0) = \Theta(2\pi), \quad \Theta'(0) = \Theta'(2\pi) \quad (2.3.7)$$

$$r^2 R'' + r R' + (\lambda r^2 - \nu) R = 0, \quad R'(a) = 0 \quad (2.3.8)$$

The Angle Function. Looking at equation (2.3.7), since we know that Θ is periodic with period 2π , its derivative must also be periodic of period 2π . This explains the choice for the boundary condition.

- Case 1: $\nu = 0$. The equation becomes $\Theta'' = 0$. The general solution to this DE is $\Theta = A\theta + B$. The condition $\Theta(0) = \Theta(2\pi)$ implies that $2A\pi = 0$, or $A = 0$. The other condition is free. This means that ν_0 must be an eigenvalue and the function $\Theta_0(\theta) = 1$ is the corresponding eigenfunction.
- Case 2: $\nu < 0$. Let $\nu = -p^2$. Equation (2.3.7) becomes

$$\Theta'' - p^2 \Theta = 0. \quad (2.3.9)$$

The solution to this equation is $\Theta = A \cosh(p\theta) + B \sinh(p\theta)$. The derivative is $\Theta' = p[A \sinh(p\theta) + B \cosh(p\theta)]$. The two boundary conditions $\Theta(0) = \Theta(2\pi)$, $\Theta'(0) = \Theta'(2\pi)$ gives

$$\begin{aligned} A &= A \cosh(2\pi p) + B \sinh(2\pi p) \\ Bp &= p[A \sinh(2\pi p) + B \cosh(2\pi p)] \end{aligned}$$

Simplify, and summing these two equations gives

$$(A + B) = (A + B) \cosh(2\pi p) + (A + B) \sinh(2\pi p) \quad (2.3.10)$$

Simplify again and we'll have

$$\cosh(2p\pi) + \sinh(2p\pi) = e^{2p\pi} = 1 \Rightarrow p = 0 \quad (2.3.11)$$

This contradicts our choice of eigenvalue and therefore, no eigenfunctions.

- Case 3: $\nu > 0$. Let $\nu = p^2$. The BVP (2.3.7) becomes $\Theta'' + p^2 \Theta = 0$, $\Theta(0) = \Theta(2\pi)$, $\Theta'(0) = \Theta'(2\pi)$. The solution to this DE is $\Theta = A \cos(p\theta) + B \sin(p\theta)$. Since Θ is periodic of period 2π , this solution always holds true. Let $\nu = n^2$, $n = 0, 1, 2, \dots$. We now have

$$\nu_n = n^2, \quad n = 0, 1, \dots \quad (2.3.12)$$

as our family of eigenvalues, and

$$\Theta_n(\theta) = a_n \cos(n\theta) + b_n \sin(n\theta) \quad (2.3.13)$$

are the eigenfunctions.

The Radius Function. Recall that $\nu = n^2$, $n = 0, 1, 2, \dots$

- Case 1: $\lambda > 0$. Let $\lambda = p^2$. Equation (2.3.8) becomes

$$r^2 R'' + rR' + (p^2 r^2 - n^2)R = 0, \quad R'(a) = 0, \quad 0 < r < a$$

The Sturm-Liouville form of this equation is

$$\frac{1}{r} \left[(rR')' - \frac{n^2}{r} R \right] + \lambda R = 0, \quad 0 < r < a. \quad (2.3.14)$$

Since we have $w(r) = r$ becomes zero at $r = 0$, this is a singular Sturm-Liouville problem.

Let $r = x/p$ and let $z(x) = R(x/p)$. Thus,

$$R = z, \quad R' = \frac{p}{x} z', \quad R'' = \frac{p^2}{x^2} z' \quad (2.3.15)$$

Since this is a singular Sturm-Liouville problem, we can modify the boundary condition and obtain the actual Bessel equation and its boundary condition to be:

$$x^2 z''(x) + xz(x) + (x^2 - n^2)z(x) = 0, \quad z, z' \text{ bounded as } x \rightarrow 0^+ \quad (2.3.16)$$

The solutions to this differential equation are the Bessel functions of the first and second kinds,

$$z_n = c_1 J_n(x) + c_2 Y_n(x), \quad (2.3.17)$$

where

$$J_n(x) = \sum_{k=0}^{\infty} \frac{(-1)^k}{k! \Gamma(1+n+k)} \left(\frac{x}{2}\right)^{2k+n} \quad \text{and}, \quad Y_n(x) = \frac{J_n(x) \cos(p\pi) - J_{-n}(x)}{\sin(n\pi)} \quad (2.3.18)$$

We need to take note of the function $Y_n(x)$. The reason why $Y_n(x)$ are special is illustrated in the graphs below:

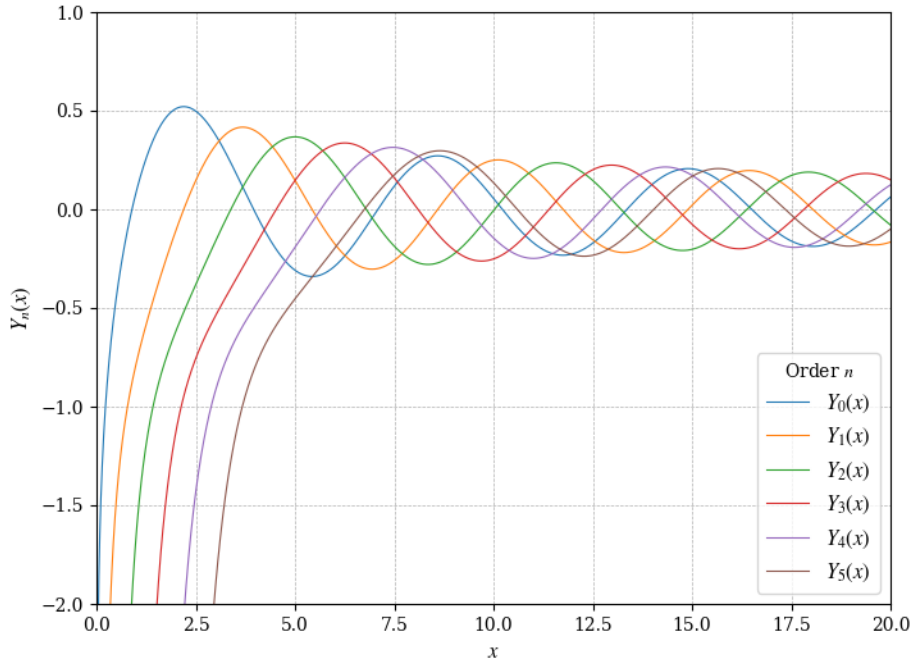


Figure 2.1: First five Bessel functions of the second kind, $Y_n(x)$.

Since $Y_n(x) \rightarrow -\infty$ as $x = pr \rightarrow 0^+$, which does not make sense (the height of the plate cannot be infinity), it must be the case that $c_2 = 0$. Converting back to $R_n(r)$ form, we obtain

$$R_n(r) = J_n(x) = J_n(pr) \quad (2.3.19)$$

The derivative of the Bessel function is proven to be

$$\frac{d}{dx} J_n(x) = \frac{J_{n-1}(x) - J_{n+1}(x)}{2} \quad (2.3.20)$$

Going back to the boundary condition $R'_n(a) = 0$, thus

$$J_{n-1}(x) = J_{n+1}(x) \quad \text{or}, \quad \sum_{k=0}^{\infty} \frac{(-1)^k}{k! \Gamma(n+k)} \left(\frac{x}{2}\right)^{2k+n-1} = \sum_{k=0}^{\infty} \frac{(-1)^k}{k! \Gamma(2+n+k)} \left(\frac{x}{2}\right)^{2k+n+1}, \quad (2.3.21)$$

The goal here is to find p such that $R'(a) = J'_n(pa) = 0$. This means that pa must be the zeroes of $J'_n(x) = \frac{1}{2}[J_{n-1}(x) - J_{n+1}(x)]$. Let z_{nm} denote the m th zero of the n th order Bessel function $J_n(x)$. Then, $p_{nm}a = z_{nm}$, or $\sqrt{\lambda_{nm}} = z_{nm}/a$. All eigenvalues of this problem is

$$\lambda_{nm} = \left(\frac{z_{nm}}{a}\right)^2, \quad n = 0, 1, 2, \dots, m = 1, 2, \dots \quad (2.3.22)$$

The corresponding eigenfunction is, therefore,

$$R_{nm}(r) = J_n\left(\sqrt{\lambda_{nm}}r\right) = J_n\left(\frac{z_{nm}r}{a}\right) \quad (2.3.23)$$

- Case 2: $\lambda < 0$. Let $\lambda = -p^2$. Equation (2.3.8) becomes

$$r^2 R'' + rR' - (p^2 r^2 + n^2)R = 0, \quad R'(a) = 0, \quad 0 < r < a \quad (2.3.24)$$

Do the same trick all over again and let $r = x/p$, we obtain the Modified Bessel Function with a new set of boundary conditions:

$$x^2 z''(x) + xz(x) - (x^2 + n^2)z(x) = 0, \quad z, z' \text{ bounded as } x \rightarrow 0^+. \quad (2.3.25)$$

The solutions to this equation are the Modified Bessel Function of the first and second kind,

$$z_n = c_1 I_n(x) + c_2 K_n(x). \quad (2.3.26)$$

Just like its cousin, the functions $K_n(x)$ are also singular at $x = 0$. For a better visualization, their graphs are illustrated below:

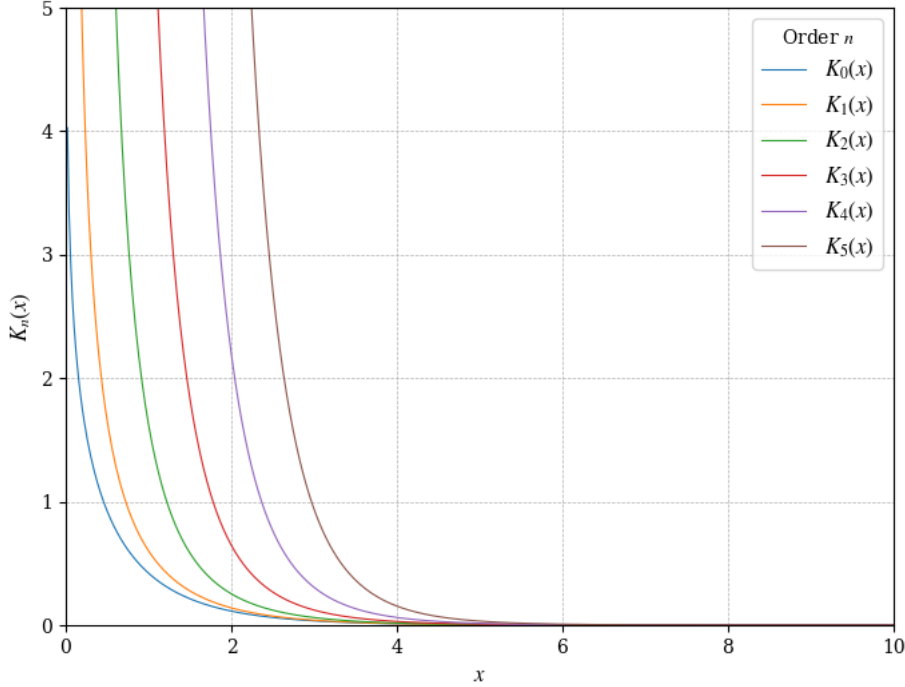


Figure 2.2: First five modified Bessel functions of the second kind, $K_n(x)$.

The second modified Bessel function $K_n(x) \rightarrow +\infty$ as $x \rightarrow 0^+$. Therefore, the modified boundary condition forces $c_2 = 0$. This left us with the remaining one. Converting back to $R_n(r)$, we obtain

$$R_n(r) = I_n(pr). \quad (2.3.27)$$

The goal here remains the same, to find all $p = \sqrt{\lambda}$ such that $R'_n(a) = I'_n(pa) = 0$. However, note that

$$I_n(x) = \sum_{k=0}^{\infty} \frac{1}{k! \Gamma(1+n+k)} \left(\frac{x}{2}\right)^{2k+n} \Rightarrow I'_n(x) = \sum_{k=1}^{\infty} \frac{1}{k! \Gamma(1+n+k)} \frac{2k+n}{2} \left(\frac{x}{2}\right)^{2k+n-1} \quad (2.3.28)$$

The derivative of $I'_n(x)$ is a monotonically increasing function, and it has its only zero at $x = 0$, or $pa = 0$, which contradicts our choice of λ , therefore its eigenvalue cannot exist.

- Case 3: $\lambda = 0$ Equation (2.3.8) becomes

$$r^2 R'' + r R' - n^2 R = 0, \quad R'(a) = 0, \quad 0 < r < a. \quad (2.3.29)$$

This is our beloved Cauchy-Euler equation, and therefore its solution is

$$R_n(r) = c_1 r^n + c_2 r^{-n} \quad (2.3.30)$$

The Sturm-Liouville form of this equation is

$$\frac{1}{e^{-1/r}} [(r e^{-1/r} R') - n^2 y] = 0 \quad (2.3.31)$$

Clearly, $1/e^{-1/r} = e^{1/r} \rightarrow +\infty$ as $r \rightarrow 0^+$. Thus, $x = 0$ is a singularity, and this is again, a singular Sturm-Liouville equation. The solution $r^{-n} \rightarrow +\infty$ as $r \rightarrow 0^+$. Therefore, just as

before, we modify the boundary condition to be R, R' bounded as $r \rightarrow 0^+$. This forces c_2 to be 0. The boundary condition of $R'(a) = 0$ means that

$$na^{n-1} = 0 \Rightarrow n = 0, \quad (2.3.32)$$

If this is the case, then $\lambda = 0$ is an eigenvalue, and its corresponding eigenfunction is $R(r) = 1$. Combining with the first case (the angle function) gives us the same constant eigenfunction.

The Time Function. Excluding the $\lambda = 0$ case by combining it with the constant eigenfunction from the angle function, we now only have $\lambda > 0$. Therefore, we can now jump straight to the solution of the equation

$$T'' + \lambda c^2 T = 0 \quad (2.3.33)$$

to be

$$T_{nm}(t) = A_{nm} \cos(c\sqrt{\lambda_{nm}}t) + B_{nm} \sin(c\sqrt{\lambda_{nm}}t), \quad (2.3.34)$$

where

$$\lambda_{nm} = \left(\frac{z_{nm}}{a}\right)^2, \quad n = 0, 1, 2, \dots, m = 1, 2, \dots$$

and z_{nm} are the zeroes of the derivative of the n th order Bessel function.

Combining the Solution. By combining the functions we obtained above, one solution to this DE is

$$u(r, \theta, t) = R_{nm}(r)\Theta_n(t)T_{nm}(t) \quad (2.3.35)$$

where

$$R_{nm}(r) = J_n(\sqrt{\lambda_{nm}}r) \quad (2.3.36)$$

$$\Theta_n(t) = a_{nm} \cos(n\theta) + b_{nm} \sin(n\theta) \quad (2.3.37)$$

$$T_{nm}(t) = A_{nm} \cos(c\sqrt{\lambda_{nm}}t) + B_{nm} \sin(c\sqrt{\lambda_{nm}}t) \quad (2.3.38)$$

All the functions above are defined at $n = 0$. Therefore we can put them into a separate power series (also note that $\Theta_0(t) = 1$). By the principle of superposition, the general solution to this PDE is

$$u(r, \theta, t) = \sum_{m=1}^{\infty} J_0(\sqrt{\lambda_{0m}}r) T_{0m}(t) + \sum_{n=1}^{\infty} \sum_{m=1}^{\infty} R_{nm}(r)\Theta_n(t)T_{nm}(t) \quad (2.3.39)$$

Note that 0 is a zero of all the Bessel functions. Therefore, we can add $m = 0$ to our list of zeroes z_{nm} and obtain our general solution to be

$$u(r, \theta, t) = \sum_{n=0}^{\infty} \sum_{m=0}^{\infty} R_{nm}(r)\Theta_n(\theta)T_{nm}(t), \quad n, m = 0, 1, 2, \dots \quad (2.3.40)$$

The Coefficients. Apply the initial condition $u(r, \theta, 0)$, we obtain

$$u(r, \theta, 0) = \sum_{n=0}^{\infty} \sum_{m=0}^{\infty} J_n(\sqrt{\lambda_{nm}}r) [a_{nm} \cos(n\theta) + b_{nm} \sin(n\theta)] A_{nm} = f(r, \theta) \quad (2.3.41)$$

It can be proven that the eigenfunctions do form an orthogonal family in the space $L_w^2[0, a]$, where the weight function is $w(r) = r$. Based on the theory of singular Sturm-Liouville problems, the coefficient c_{nm} is determined by

$$\begin{aligned} A_{nm}a_{nm} &= \frac{\langle J_0 \cos(n\theta), f \rangle_w}{\langle J_0, J_0 \rangle_w} = \frac{\int_0^a \int_0^{2\pi} J_n(\sqrt{\lambda_{nm}}r) \cos(n\theta) f(r, \theta) r dr d\theta}{\int_0^a \int_0^{2\pi} J_n^2(\sqrt{\lambda_{nm}}r) r dr d\theta}, \quad n, m = 0, 1, \dots \\ A_{nm}b_{nm} &= \frac{\langle J_0 \sin(n\theta), f \rangle_w}{\langle J_0, J_0 \rangle_w} = \frac{\int_0^a \int_0^{2\pi} J_n(\sqrt{\lambda_{nm}}r) \sin(n\theta) f(r, \theta) r dr d\theta}{\int_0^a \int_0^{2\pi} J_n^2(\sqrt{\lambda_{nm}}r) r dr d\theta}, \quad n, m = 0, 1, \dots \end{aligned} \quad (2.3.42)$$

Apply the other initial condition:

$$u_t(r, \theta, 0) = \sum_{n=0}^{\infty} \sum_{m=0}^{\infty} J_n(\sqrt{\lambda_{nm}}r) [a_{nm} \cos(n\theta) + b_{nm} \sin(n\theta)] B_{nm} \sqrt{\lambda_{nm}} c = g(r, \theta)$$

Do the same thing all over again, and let $\omega = \sqrt{\lambda_{nm}}c$

$$\begin{aligned} B_{nm}a_{nm} &= \frac{\langle J_0 \cos(n\theta), g \rangle_w}{\omega \langle J_0, J_0 \rangle_w} = \frac{\int_0^a \int_0^{2\pi} J_n(\sqrt{\lambda_{nm}}r) \cos(n\theta) g(r, \theta) r dr d\theta}{\omega \int_0^a \int_0^{2\pi} J_n^2(\sqrt{\lambda_{nm}}r) r dr d\theta}, \quad n, m = 0, 1, \dots \\ B_{nm}b_{nm} &= \frac{\langle J_0 \sin(n\theta), g \rangle_w}{\omega \langle J_0, J_0 \rangle_w} = \frac{\int_0^a \int_0^{2\pi} J_n(\sqrt{\lambda_{nm}}r) \sin(n\theta) g(r, \theta) r dr d\theta}{\omega \int_0^a \int_0^{2\pi} J_n^2(\sqrt{\lambda_{nm}}r) r dr d\theta}, \quad n, m = 0, 1, \dots \end{aligned} \quad (2.3.43)$$

Go back to the wave function:

$$\begin{aligned} u(r, \theta, 0) &= \sum_{n,m=0}^{\infty} J_n(\sqrt{\lambda_{nm}}r) [a_{nm} \cos(n\theta) + b_{nm} \sin(n\theta)] [A_{nm} \cos(\omega t) + B_{nm} \sin(\omega t)] \\ &= \sum_{n,m=0}^{\infty} J_n(\sqrt{\lambda_{nm}}r) [a_{nm} \cos(n\theta) + b_{nm} \sin(n\theta)] A_{nm} \cos(\omega t) \\ &\quad + \sum_{n,m=0}^{\infty} J_n(\sqrt{\lambda_{nm}}r) [a_{nm} \cos(n\theta) + b_{nm} \sin(n\theta)] B_{nm} \sin(\omega t) \end{aligned} \quad (2.3.44)$$

Plugging in $a_{nm}A_{nm}$, $b_{nm}A_{nm}$ from (2.3.42) into the first sum, and $a_{nm}B_{nm}$, $b_{nm}B_{nm}$ from (2.3.43) into the second sum, A_{nm} and B_{nm} will be canceled out. The final step is to redefine a_{nm} to be $a_{nm}A_{nm}$, b_{nm} to be $b_{nm}A_{nm}$, c_{nm} to be $a_{nm}B_{nm}$, and d_{nm} to be $b_{nm}B_{nm}$. It is also not hard to notice that $k = \sqrt{\lambda_{nm}} = z_{nm}/a$. Thus, the complementary solution is

$$u(r, \theta, 0) = \sum_{n=0}^{\infty} \sum_{m=0}^{\infty} J_n\left(\frac{z_{nm}r}{a}\right) [\Psi_{nm}(\theta) \cos(\omega t) + \Phi_{nm}(\theta) \sin(\omega t)], \quad (2.3.45)$$

where

$$\Psi_{nm}(\theta) = a_{nm} \cos(n\theta) + b_{nm} \sin(n\theta) \quad (2.3.46)$$

$$\Phi_{nm}(\theta) = c_{nm} \cos(n\theta) + d_{nm} \sin(n\theta) \quad (2.3.47)$$

$$\omega = \frac{cz_{nm}}{a} = ck \quad (2.3.48)$$

and,

$$a_{nm} = \frac{\langle J_0 \cos(n\theta), f \rangle_w}{\langle J_0, J_0 \rangle_w} = \frac{\int_0^a \int_0^{2\pi} J_n(kr) \cos(n\theta) f(r, \theta) r dr d\theta}{2\pi \int_0^a J_n^2(kr) r dr}, \quad n, m = 0, 1, \dots \quad (2.3.49)$$

$$b_{nm} = \frac{\langle J_0 \sin(n\theta), f \rangle_w}{\langle J_0, J_0 \rangle_w} = \frac{\int_0^a \int_0^{2\pi} J_n(kr) \sin(n\theta) f(r, \theta) r dr d\theta}{2\pi \int_0^a J_n^2(kr) r dr}, \quad n, m = 0, 1, \dots \quad (2.3.50)$$

$$c_{nm} = \frac{\langle J_0 \cos(n\theta), g \rangle_w}{\omega \langle J_0, J_0 \rangle_w} = \frac{\int_0^a \int_0^{2\pi} J_n(kr) \cos(n\theta) g(r, \theta) r dr d\theta}{2\pi \omega \int_0^a J_n^2(kr) r dr}, \quad n, m = 0, 1, \dots \quad (2.3.51)$$

$$d_{nm} = \frac{\langle J_0 \sin(n\theta), g \rangle_w}{\omega \langle J_0, J_0 \rangle_w} = \frac{\int_0^a \int_0^{2\pi} J_n(kr) \sin(n\theta) g(r, \theta) r dr d\theta}{2\pi \omega \int_0^a J_n^2(kr) r dr}, \quad n, m = 0, 1, \dots \quad (2.3.52)$$

General Solution. Suppose the general solution can be written as

$$u(r, \theta, t) = u_1 + u_2 = \sum_{n,m} \eta_1(r, \theta) y_1(t) + \eta_2(r, \theta) y_2(t) \quad (2.3.53)$$

Differentiating with respect to time:

$$\frac{\partial^2 u_1}{\partial t^2} = \sum_{n,m} \eta_1(r, \theta) \frac{d^2 y_1}{dt^2} \quad \text{and} \quad \frac{\partial^2 u_2}{\partial t^2} = \sum_{n,m} \eta_2(r, \theta) \frac{d^2 y_2}{dt^2} \quad (2.3.54)$$

Again, since

$$\nabla^2 \eta_1 = R_1 \Theta_1 \left(\frac{R''}{R} + \frac{1}{r} \frac{R'}{R} + \frac{1}{r^2} \frac{\Theta''}{\Theta} \right) = -\lambda_{nm}^{(1)} R_1 \Theta_1 \quad (2.3.55)$$

$$\nabla^2 \eta_2 = R_2 \Theta_2 \left(\frac{R''}{R} + \frac{1}{r} \frac{R'}{R} + \frac{1}{r^2} \frac{\Theta''}{\Theta} \right) = -\lambda_{nm}^{(1)} R_2 \Theta_2, \quad (2.3.56)$$

Also split Q into $Q_1 + Q_2$. Same process again,

$$\frac{\partial^2 u_i}{\partial t^2} - c^2 \nabla^2 u_i = Q_i(r, \theta, t) \implies \sum_{m,n} \left(\frac{d^2 y_i}{dt^2} + c^2 \lambda_{nm} y_i \right) \eta_i = Q_i(r, \theta, t), \quad i = 1, 2 \quad (2.3.57)$$

Expand Q in terms of eigenfunctions,

$$Q_1(r, \theta, t) = \sum_{n,m \geq 1} p_{nm} \eta_1(r, \theta), \quad \text{and} \quad Q_2(r, \theta, t) = \sum_{n,m \geq 1} q_{nm} \eta_2(r, \theta) \quad (2.3.58)$$

where

$$p_{nm}(t) = \frac{\iint_{\Omega} Q(r, \theta, t) \eta_1(r, \theta) r dr d\theta}{\iint_{\Omega} \eta_1^2(r, \theta) r dr d\theta} \quad \text{and} \quad q_{nm}(t) = \frac{\iint_{\Omega} Q(r, \theta, t) \eta_2(r, \theta) dx dy}{\iint_{\Omega} \phi_{nm}^2(r, \theta) r dr d\theta} \quad (2.3.59)$$

Here, $\Omega = \{(r, \theta) \mid 0 \leq r \leq a', 0 \leq \theta \leq 2\pi\}$, and $\eta_1(r, \theta) = J_n(r) \Psi(\theta)$, $\eta_2(r, \theta) = J_n(r) \Phi(\theta)$.

Final Solution. Equating two equations gives, and solves by variation of parameters, we obtain the general solution to be

$$u(r, \theta, t) = \sum_{n=0}^{\infty} \sum_{m=0}^{\infty} J_n(kr) [\Psi_{nm}(\theta) y_1(t) + \Phi_{nm}(\theta) y_2(t)], \quad (2.3.60)$$

where

$$\Psi_{nm}(\theta) = a_{nm} \cos(n\theta) + b_{nm} \sin(n\theta) \quad (2.3.61)$$

$$\Phi_{nm}(\theta) = c_{nm} \cos(n\theta) + d_{nm} \sin(n\theta) \quad (2.3.62)$$

$$y_1(t) = \alpha \cos(\omega t) + \beta \sin(\omega t) + \int_0^t p_{nm}(\tau) \frac{\sin(\omega(t-\tau))}{\omega} d\tau \quad (2.3.63)$$

$$y_2(t) = \gamma \cos(\omega t) + \sigma \sin(\omega t) + \int_0^t q_{nm}(\tau) \frac{\sin(\omega(t-\tau))}{\omega} d\tau \quad (2.3.64)$$

$$\omega = \frac{cz_{nm}}{a} = ck \quad (2.3.65)$$

Here, $\alpha, \beta, \gamma, \sigma$ are arbitrary constants that satisfies $\alpha + \gamma = 1$, $\beta + \sigma = 1$, and $\alpha^2 + \gamma^2 \neq 0$, $\beta^2 + \sigma^2 \neq 0$, and,

$$a_{nm} = \frac{\langle J_0 \cos(n\theta), f \rangle_w}{\langle J_0, J_0 \rangle_w} = \frac{\int_0^a \int_0^{2\pi} J_n(kr) \cos(n\theta) f(r, \theta) r dr d\theta}{2\pi \int_0^a J_n^2(kr) r dr}, \quad n, m = 0, 1, \dots \quad (2.3.66)$$

$$b_{nm} = \frac{\langle J_0 \sin(n\theta), f \rangle_w}{\langle J_0, J_0 \rangle_w} = \frac{\int_0^a \int_0^{2\pi} J_n(kr) \sin(n\theta) f(r, \theta) r dr d\theta}{2\pi \int_0^a J_n^2(kr) r dr}, \quad n, m = 0, 1, \dots \quad (2.3.67)$$

$$c_{nm} = \frac{\langle J_0 \cos(n\theta), g \rangle_w}{\omega \langle J_0, J_0 \rangle_w} = \frac{\int_0^a \int_0^{2\pi} J_n(kr) \cos(n\theta) g(r, \theta) r dr d\theta}{2\pi \omega \int_0^a J_n^2(kr) r dr}, \quad n, m = 0, 1, \dots \quad (2.3.68)$$

$$d_{nm} = \frac{\langle J_0 \sin(n\theta), g \rangle_w}{\omega \langle J_0, J_0 \rangle_w} = \frac{\int_0^a \int_0^{2\pi} J_n(kr) \sin(n\theta) g(r, \theta) r dr d\theta}{2\pi \omega \int_0^a J_n^2(kr) r dr}, \quad n, m = 0, 1, \dots \quad (2.3.69)$$

Chapter 3

Designing the Plotting Algorithm

3.1 The Square Plate

The reason for all those derivations above is to plot our theoretical patterns. Recall that our final solution is determined by

$$u(x, y, t) = \frac{1}{4}A_{00} + \sum_{n=1}^{\infty} \sum_{m=1}^{\infty} X_n(x)Y_m(y)W_{nm}(t), \quad (3.1.1)$$

where

$$X_n(x) = a_n \cos\left(\frac{n\pi x}{L}\right) + \bar{a}_n \sin\left(\frac{n\pi x}{L}\right) \quad (3.1.2)$$

$$Y_m(y) = a_m \cos\left(\frac{m\pi y}{L}\right) + \bar{a}_m \sin\left(\frac{m\pi y}{L}\right) \quad (3.1.3)$$

$$W_{nm}(t) = A_{nm} \cos(\omega t) + B_{nm} \sin(\omega t) + \int_0^t q_{nm}(\tau) \frac{\sin(\omega t - \omega\tau)}{\omega} d\tau \quad (3.1.4)$$

$$\omega = \frac{\pi}{L} c \sqrt{n^2 + m^2} \quad (3.1.5)$$

and,

$$A_{nm} = \frac{4}{L^2} \int_{-L/2}^{L/2} \int_{-L/2}^{L/2} f(x, y) X_n(x) Y_m(y) dx dy, \quad n, m = 0, 1, 2, \dots \quad (3.1.6)$$

$$B_{nm} = \frac{4}{L^2} \int_{-L/2}^{L/2} \int_{-L/2}^{L/2} \frac{g(x, y)}{\omega} X_n(x) Y_m(y) dx dy, \quad n, m = 1, 2, 3, \dots \quad (3.1.7)$$

In order to plot the shapes, there are a few things to note:

- In realistic conditions, there is no way to find what the initial functions $f(x, y)$ and $g(x, y)$ are. However, we can assume that the initial velocity is zero ($g(x, y) = 0$). Also, notice that the forcing term is non-zero only when $n = m$, and it also approaches zero as $\omega \rightarrow \infty$, therefore it does not matter that much for the shape of the plot. Our wave equation is now simplified to

$$u(x, y, t) = \sum_{n=0}^{\infty} \sum_{m=0}^{\infty} X_n(x) Y_m(y) A_{nm} \cos(\omega t) \quad (3.1.8)$$

- For $f(x, y)$, we can choose a function $f(x, y)$ such that

$$|A_{ij}| \approx |A_{nm}|, \quad (3.1.9)$$

for any $(i, j) \neq (n, m)$. We can do this because, in reality, the amplitude of the plate is extremely small, so the choice of function, $f(x, y)$ does not matter that much, as long as $f(x, y) \neq 0$.

- What we are really interested in the shape of the nodal lines, so we can input certain time points such that $\cos(\omega t) = 1$ ($t = 0, 2\pi/\omega, 4\pi/\omega, \dots$). In this way, the coefficient we choose, A_{nm} can be cancelled out, and we are left with

$$u(x, y, t) = \sum_{n=0}^{\infty} \sum_{m=0}^{\infty} X_n(x) Y_m(y) \quad (3.1.10)$$

- One final thing to note is that the general solution that we derived, $u(x, y, t_0)$ is the superposition sum of all other possible solutions, but what we're interested in are solutions at certain frequencies. Recall that

$$\omega = \frac{\pi c}{L} \sqrt{n^2 + m^2}. \quad (3.1.11)$$

This means that each ω corresponds to only a few set of n and m . For example, if $\omega = \frac{\pi c}{L} \sqrt{5}$, then all the possible combinations of n and m are $(1, 2)$ and $(2, 1)$. Note that we used the absolute values for the coefficient, this implies that negative coefficients are possible. The two equations that describe the Chladni pattern found at this frequency are

$$X_1(x)Y_2(y) + X_2(x)Y_1(y) = 0, \quad \text{and} \quad X_1(x)Y_2(y) - X_2(x)Y_1(y) = 0, \quad (3.1.12)$$

For equations with more sum of squares combinations, there will be more combinations for a single mode. For example, for $\omega = \frac{\pi c}{L} \sqrt{65}$, all the possible implicit functions are

$$X_1(x)Y_8(y) \pm X_4(x)Y_7(y) \pm X_7(x)Y_4(y) \pm X_8(x)Y_1(y) = 0 \quad (3.1.13)$$

We need not consider the first term due to symmetry. In general, if there are N terms in the equation, there will be a total of 2^{N-1} possible plots.

- ***Special Cases:** If $n^2 + m^2$ is a perfect square $(1, 4, 9, 16, 25, \dots)$, then we also need to consider the pairs with 0. For example, if $n^2 + m^2 = 25$, then besides the standard pairs of $(3, 4)$ and $(4, 3)$, we also need to consider the pairs $(0, 5)$ and $(5, 0)$. This is because since we don't know what $f(x, y)$ is, we also don't know whether A_{00} is 0. If it's zero, then we just plot the regular pairs $(3, 4)$ and $(4, 3)$,

$$X_3(x)Y_4(y) + X_4(x)Y_3(y) = 0, \quad \text{and} \quad X_3(x)Y_4(y) - X_4(x)Y_3(y) = 0. \quad (3.1.14)$$

If A_{00} is not zero, meaning that the summation actually starts at index $(n, m) = (0, 0)$, then we also need to consider eight other patterns

$$X_0(x)Y_5(y) \pm X_3(x)Y_4(y) \pm X_4(x)Y_3(y) \pm X_5(x)Y_0(y) = 0. \quad (3.1.15)$$

In total, for the case of $S = 25$, there will be a total of $2 + 8 = 10$ plots.

Implementation. To obtain the contour plot of $u(x, y, 0)$, we first need to define a basis function

```

def X(x, n):
    return np.mod(n + 1, 2) * np.cos(n * np.pi * x / 2.0)
    + np.mod(n, 2) * np.sin(n * np.pi * x / 2.0)

```

After that, we need to define a few more functions,

```

def generate_sign_combinations(pairs) # to generate different sign combinations for X

def u(x, y, pairs, signs) # plot the full wave function

def find_pairs(number) # search for numbers with sum of squares

def exist_sos(number) # Check if a given number has sums of squares pairs

```

Finally, we need to plot it using

```
def plot_sum_of_squares(start_index, end_index)
```

The full code on how to do this is included in the appendix at the end and is publicly available on [Github](#) [5].

3.2 The Circular Plate

The circular plate is a bit easier, since we don't need to design an algorithm to search for sum of squares and perfect squares exceptions. Recall that for a circular plate,

$$u(r, \theta, t) = \sum_{n=0}^{\infty} \sum_{m=0}^{\infty} J_n(kr) [\Psi_{nm}(\theta)y_1(t) + \Phi_{nm}(\theta)y_2(t)], \quad (3.2.1)$$

where

$$\Psi_{nm}(\theta) = a_{nm} \cos(n\theta) + b_{nm} \sin(n\theta) \quad (3.2.2)$$

$$\Phi_{nm}(\theta) = c_{nm} \cos(n\theta) + d_{nm} \sin(n\theta) \quad (3.2.3)$$

$$\omega = \frac{cz_{nm}}{a} = ck \quad (3.2.4)$$

and,

$$a_{nm} = \frac{\langle J_0 \cos(n\theta), f \rangle_w}{\langle J_0, J_0 \rangle_w} = \frac{\int_0^a \int_0^{2\pi} J_n(kr) \cos(n\theta) f(r, \theta) r dr d\theta}{2\pi \int_0^a J_n^2(kr) r dr}, \quad n, m = 0, 1, \dots \quad (3.2.5)$$

$$b_{nm} = \frac{\langle J_0 \sin(n\theta), f \rangle_w}{\langle J_0, J_0 \rangle_w} = \frac{\int_0^a \int_0^{2\pi} J_n(kr) \sin(n\theta) f(r, \theta) r dr d\theta}{2\pi \int_0^a J_n^2(kr) r dr}, \quad n, m = 0, 1, \dots \quad (3.2.6)$$

$$c_{nm} = \frac{\langle J_0 \cos(n\theta), g \rangle_w}{\omega \langle J_0, J_0 \rangle_w} = \frac{\int_0^a \int_0^{2\pi} J_n(kr) \cos(n\theta) g(r, \theta) r dr d\theta}{2\pi \omega \int_0^a J_n^2(kr) r dr}, \quad n, m = 0, 1, \dots \quad (3.2.7)$$

$$d_{nm} = \frac{\langle J_0 \sin(n\theta), g \rangle_w}{\omega \langle J_0, J_0 \rangle_w} = \frac{\int_0^a \int_0^{2\pi} J_n(kr) \sin(n\theta) g(r, \theta) r dr d\theta}{2\pi \omega \int_0^a J_n^2(kr) r dr}, \quad n, m = 0, 1, \dots \quad (3.2.8)$$

Do the same thing as before, we can eliminate c_{nm} , d_{nm} , and the forcing term. The circular plate is way easier to implement because we don't have to search for any sum of squares, so each Chladni pattern is simply a pair of arbitrary n and m . The equations that we need to plot are simply

$$u_{nm}(r, \theta, 0) = J_n(kr)[a_{nm} \cos(n\theta) + b_{nm} \sin(n\theta)] \quad (3.2.9)$$

There is one thing to note, however. Unlike the square plate, the coefficient that constitutes the pattern depends on the initial function $f(r, \theta)$, but after testing out various functions $f(r, \theta)$, we noticed that it doesn't actually do anything to the contour plot at $z = 0$, only the plot in three dimensions. Therefore, for this particular equation, we just choose a random function $f(r, \theta)$,

$$f(r, \theta) = r \cos(\theta) \quad (3.2.10)$$

Implementation. We define a few functions:

```
# Function to get the m-th zero of the derivative of the Bessel function of order n
def bessel_derivative_zero(n, m):
    if n == 0: #Redefine the first zero of J_0 prime to be 0
        zeros = list(jnp_zeros(n, m + 1))
        zeros.insert(0, 0)
        return zeros[m]
    else:
        # Get the m-th zero, treating first zero as the 0th zero
        return jnp_zeros(n, m + 1)[-1]

# Initial function f(r, theta)
def f(r, theta):
    return r * np.cos(theta)

# Two coefficients:
def a_nm(n, m, a)
def b_nm(n, m, a)

# Define the function J_n(z_nm * r / a) * (a_nm * cos(n*theta) + b_nm * sin(n*theta))
def u(n, m, r, theta, a)
```

and finally,

```
def plot_polar_contour(n_max, m_max, a, resolution=100)
```

The full code on how to do this is included in the appendix at the end and is publicly available on [Github](#) [5].

Chapter 4

Experiment Procedure and Results

4.1 Procedure

The experimentation of our group is fairly simple, but for documentation purposes, and for anyone who wants to do experiment in the future, a detailed list of procedures is provided below.

1. Obtain the lab equipment from the box that is labeled “Chaldni Plates”. In the box, there are a number of items that will and will not be used. Below is the list of the items that will be used.
 - Oscillator and Function Generator
 - Square and circular Chaldni plates
 - Two banana-to-banana cables
 - Pin and pin screw head
 - Bottle of sand
2. Run a simulation using Desmos, a text editor, or an IDE to program the formula that relates the 2-dimensional plate. The pattern obtained from the plate is the contour plot of the function $u(x, y, t)$ obtained above, which is

$$\sum_{m,n} X_n(x)Y_m(y) = 0 \quad \text{where } m^2 + n^2 = (2Lf/c)^2$$

For example, for $(2Lf/c)^2 = 65$, since $m^2 + n^2 = 65$ has $(1, 8)$, $(4, 7)$, $(7, 4)$, and $(8, 1)$ as ordered solutions, therefore the implicit equations that describe the pattern are

$$X_1(x)Y_8(y) \pm X_4(x)Y_7(y) \pm X_7(x)Y_4(y) \pm X_8(x)Y_1(y) = 0.$$

Here, $X_n(x)$ and $Y_m(y)$ are part of the solution to the wave equation obtained from the section above, which are

$$X_n(x) = \frac{1 + (-1)^n}{2} \cos\left(\frac{n\pi x}{L}\right) + \frac{1 - (-1)^n}{2} \sin\left(\frac{n\pi x}{L}\right), \quad n = 1, 2, 3, \dots$$
$$Y_m(y) = \frac{1 + (-1)^m}{2} \cos\left(\frac{m\pi y}{L}\right) + \frac{1 - (-1)^m}{2} \sin\left(\frac{m\pi y}{L}\right), \quad m = 1, 2, 3, \dots$$

Note that since 65 will have four pairs, so there will be $2^{4-1} = 8$ patterns from the sign alternation.

When determining m and n values for the solutions to the term $(2Lf/c)^2$, **ALL** possible combinations of perfect squares that satisfy the equation must be included in the graph for that *particular* frequency value. To assist in finding all possible combinations, run another program that finds all possible combinations of the sum of squares for some positive integer N that represents the quantity $(2Lf/c)^2$.

Note that you will most likely not get a perfect integer when experimenting. However, it is okay to round to the nearest whole number. In the case that no such m and n values exist at some particular value even after rounding up or down, round to the nearest value where at least one exists. A detailed algorithm on how to do this will be provided in the section below.

3. Measure the level of the table. The table the experiment is taking place on should be *as level as possible*. Even a fraction of a degree will skew the symmetry in the patterns obtained.
4. Measure two adjacent sides of the square plate and take the average of the two values. The average will be the value of the side of the plate. Similarly, measure the diameter of the circular plate. Record your values.
5. Set up the equipment so that it follows the setup shown in Figure 1. Make sure to look up the maximum voltage that can be applied to the oscillator so that the equipment isn't damaged. If you want to limit the amount of sand that will have to be cleaned up, place a sturdy bin underneath the setup.
6. Turn on the power supply and set it to a *safe* voltage. This voltage should be constant in the experiment, so this value should not be interchanged between data collection. Once the oscillator is on, set the frequency to 50 Hz and sprinkle sand onto the plate. Turn the knob until the plate is in resonance (a pattern arises). Record the frequency and respective pattern that arises. Find another 15-20 patterns at different unique frequencies and record your results
7. Repeat steps (5) and (6) but this time with the circular plate.
8. Clean up the station and neatly put all equipment back where it belongs.

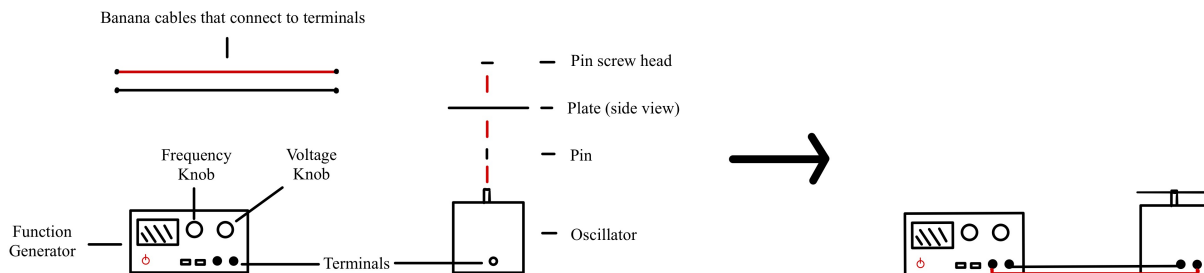


Figure 1: Follow this diagram to setup the experiment

4.2 Experimental and Theoretical Results for the Square Plate

4.2.1 Experimental Results

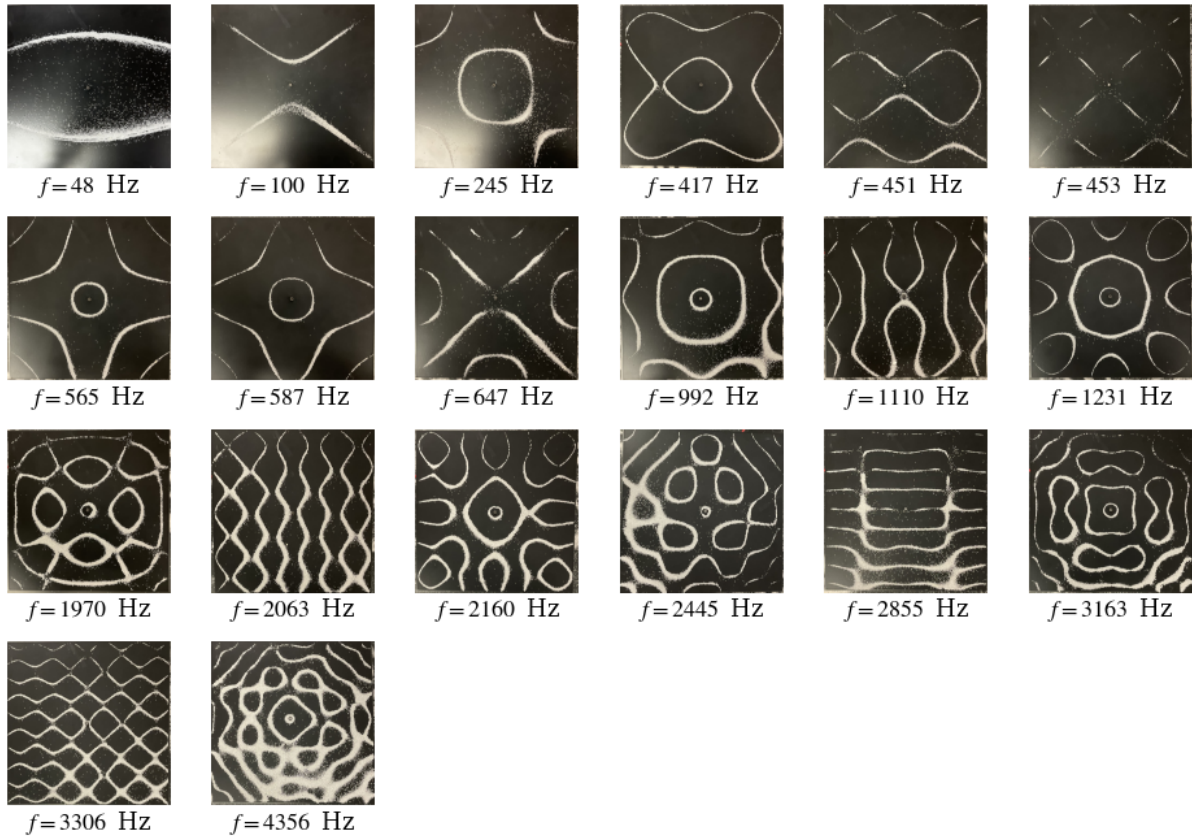


Figure 4.1: Experimental Results for the Square Plate

4.2.2 Theoretical Results

Remark. When reading the images and table below, there are a few things to notice:

- The patterns displayed above exhibit a progressive increase in frequency from left to right.
- Each pattern corresponds to a combination of different modes. All the modes of each pattern are listed in the table below.
- All patterns with the same consecutive colors are patterns of the same mode, but with different sign combinations.
- The terminology S.O.S# in the table denotes the n -th number that is a sum of square of some other numbers.

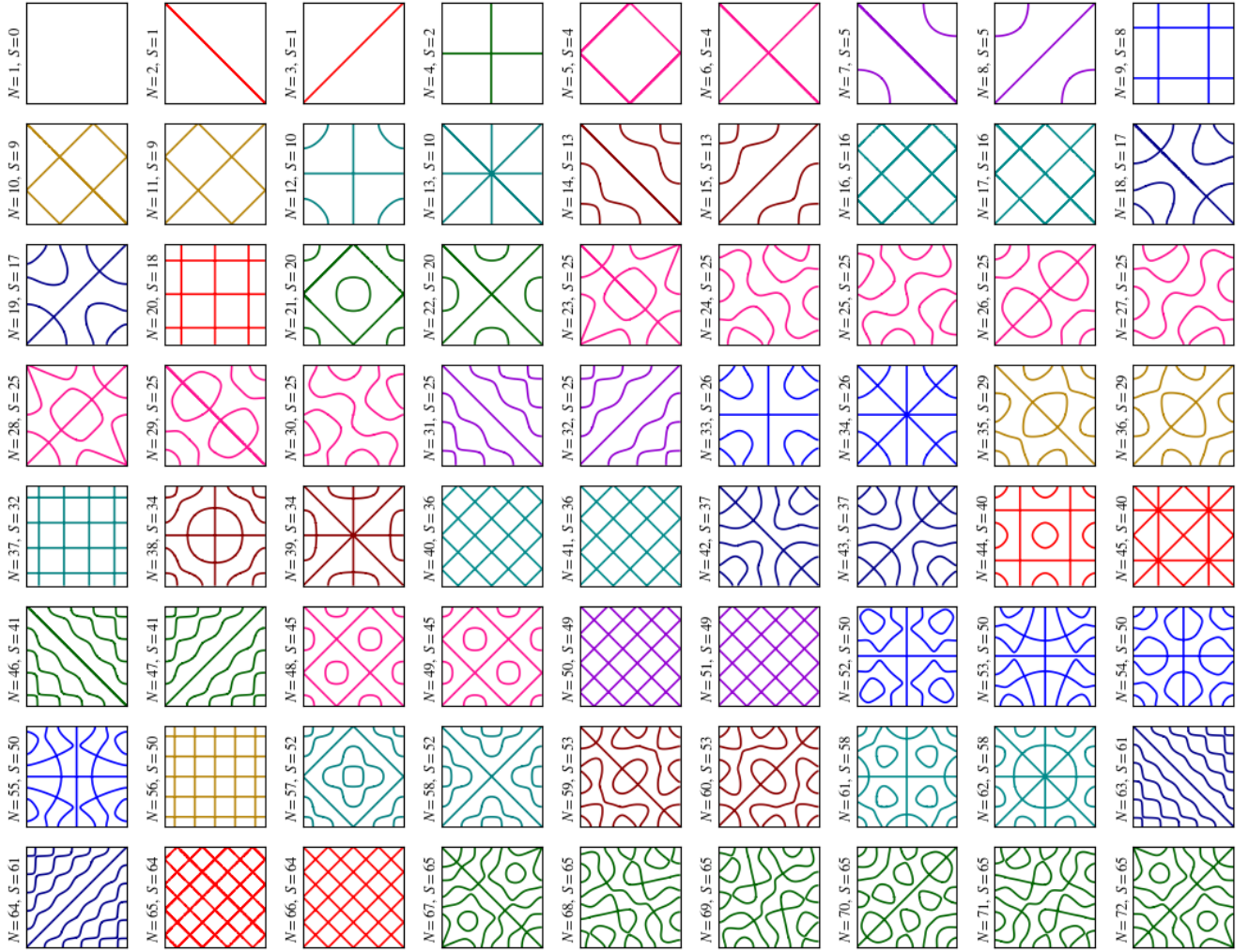


Figure 4.2: First 72 theoretical patterns of the square plate, plotted in Python.
(From the wave equation model, might not be accurate)

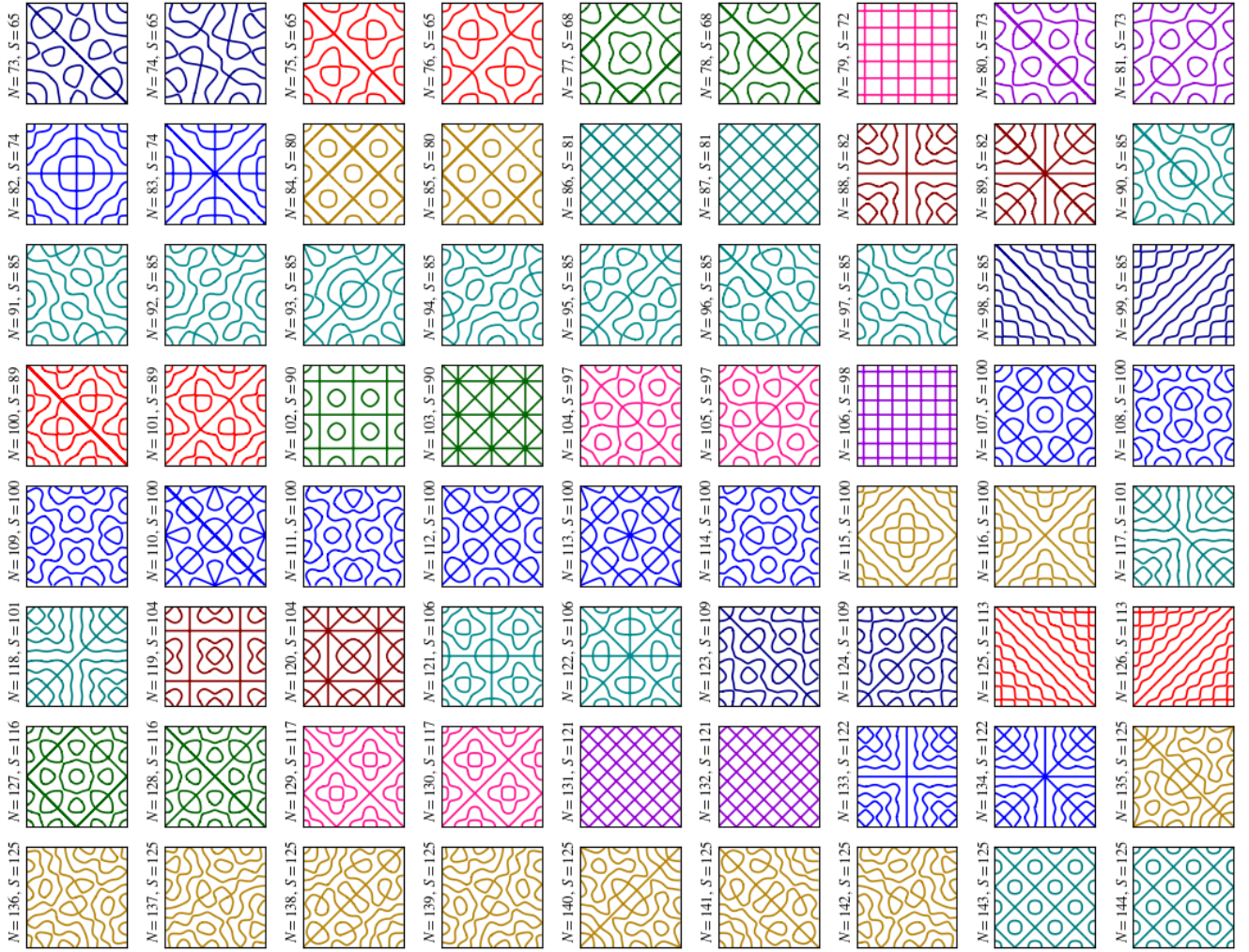


Figure 4.3: The next 72 patterns of the square plate.
(From the wave equation model, might not be accurate)

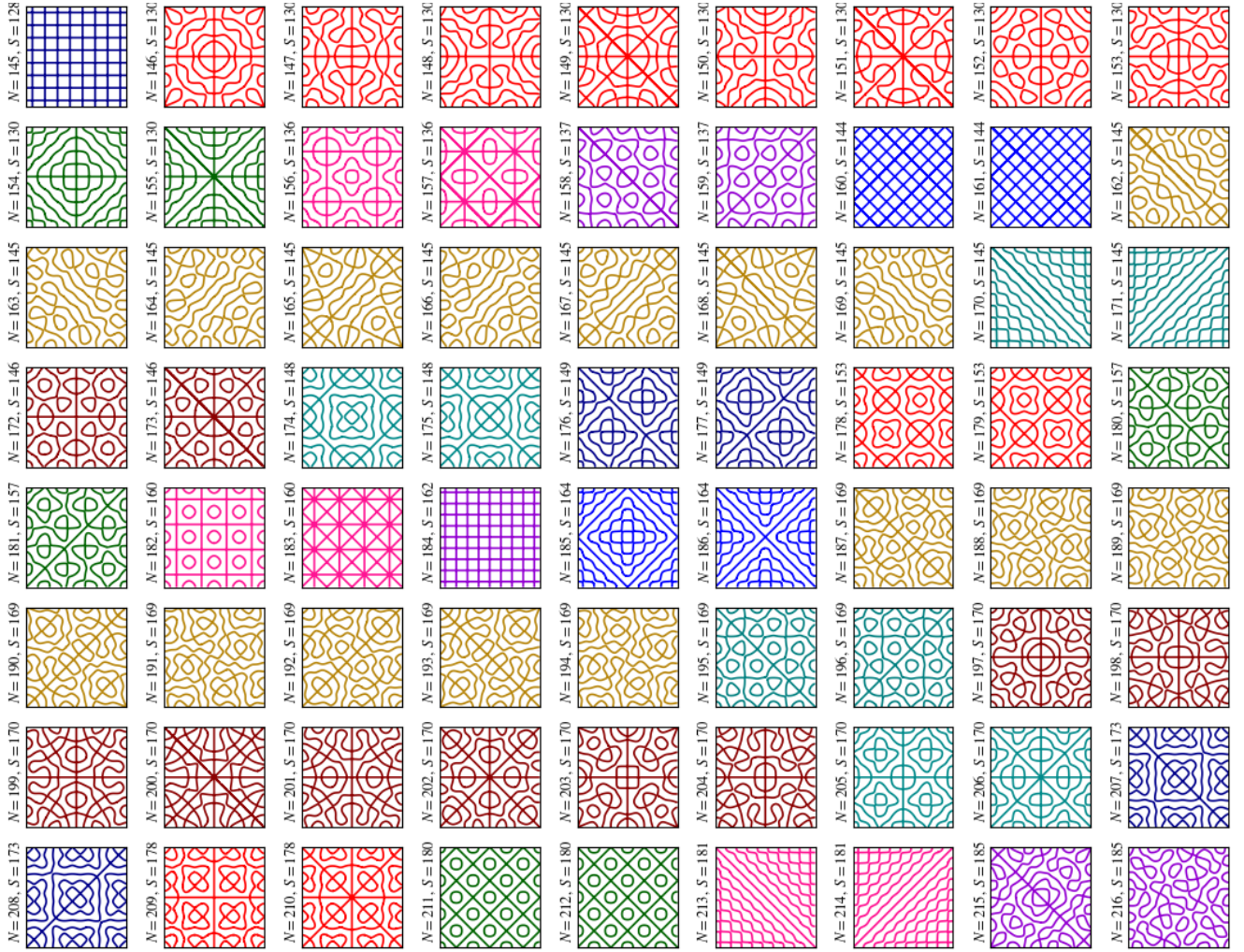


Figure 4.4: Pattern #145 to #216.
(From the wave equation model, might not be accurate)

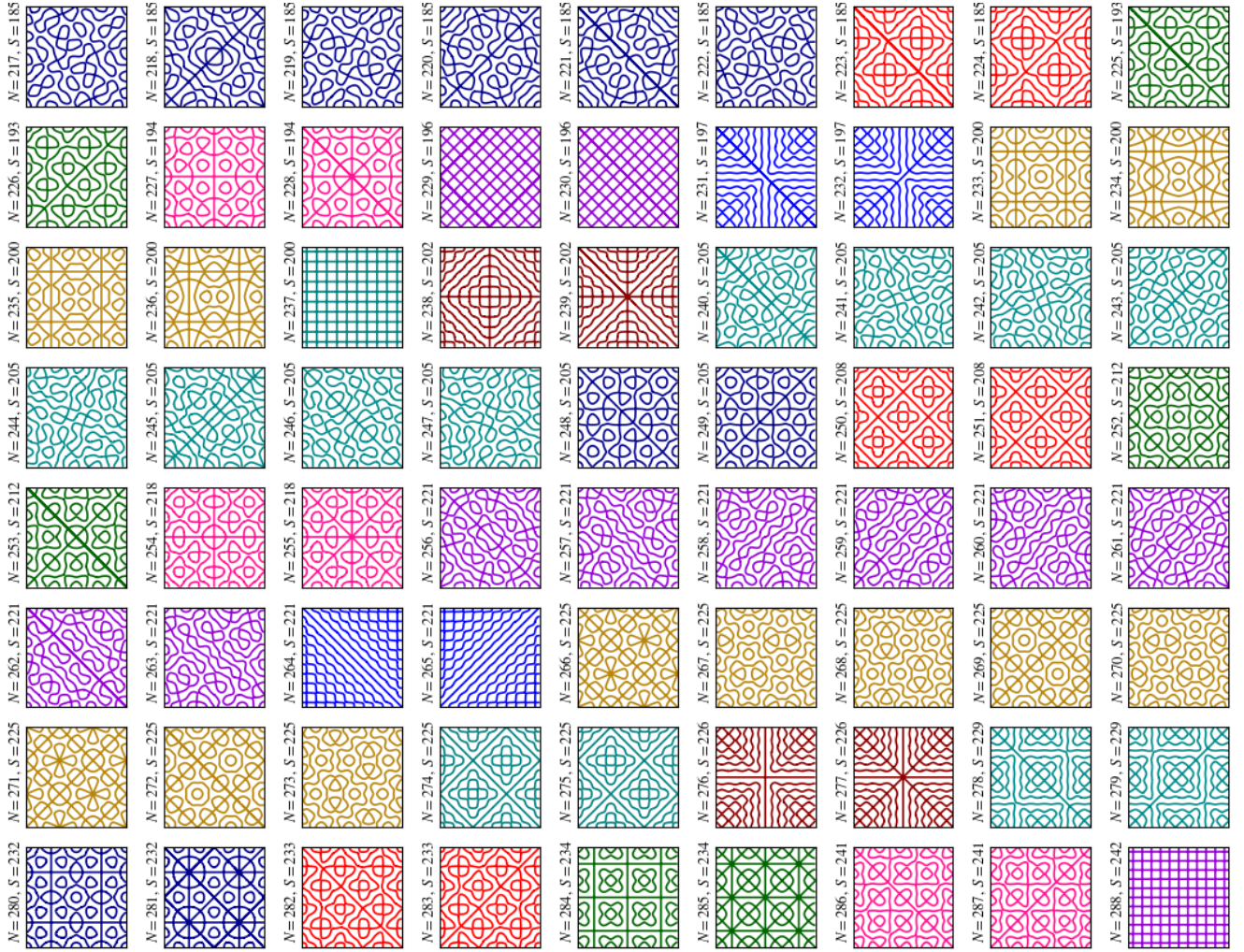


Figure 4.5: Pattern #217 to #288.
 (From the wave equation model, might not be accurate)

Table 4.1: The modes of the first 84 sum of squares numbers

S.O.S#	Sum	Modes (n, m)	S.O.S #	Sum	Modes (n, m)
1	2	(1, 1)	43	122	(1, 11) (11, 1)
2	5	(1, 2) (2, 1)	44	125	(2, 11) (5, 10) (10, 5) (11, 2)
3	8	(2, 2)	45	128	(8, 8)
4	10	(1, 3) (3, 1)	46	130	(3, 11) (7, 9) (9, 7) (11, 3)
5	13	(2, 3) (3, 2)	47	136	(6, 10) (10, 6)
6	17	(1, 4) (4, 1)	48	137	(4, 11) (11, 4)
7	18	(3, 3)	49	145	(1, 12) (8, 9) (9, 8) (12, 1)
8	20	(2, 4) (4, 2)	50	146	(5, 11) (11, 5)
9	25	(3, 4) (4, 3)	51	148	(2, 12) (12, 2)
10	26	(1, 5) (5, 1)	52	149	(7, 10) (10, 7)
11	29	(2, 5) (5, 2)	53	153	(3, 12) (12, 3)
12	32	(4, 4)	54	157	(6, 11) (11, 6)
13	34	(3, 5) (5, 3)	55	160	(4, 12) (12, 4)
14	37	(1, 6) (6, 1)	56	162	(9, 9)
15	40	(2, 6) (6, 2)	57	164	(8, 10) (10, 8)
16	41	(4, 5) (5, 4)	58	169	(5, 12) (12, 5)
17	45	(3, 6) (6, 3)	59	170	(1, 13) (7, 11) (11, 7) (13, 1)
18	50	(1, 7) (5, 5) (7, 1)	60	173	(2, 13) (13, 2)
19	52	(4, 6) (6, 4)	61	178	(3, 13) (13, 3)
20	53	(2, 7) (7, 2)	62	180	(6, 12) (12, 6)
21	58	(3, 7) (7, 3)	63	181	(9, 10) (10, 9)
22	61	(5, 6) (6, 5)	64	185	(4, 13) (8, 11) (11, 8) (13, 4)
23	65	(1, 8) (4, 7) (7, 4) (8, 1)	65	193	(7, 12) (12, 7)
24	68	(2, 8) (8, 2)	66	194	(5, 13) (13, 5)
25	72	(6, 6)	67	197	(1, 14) (14, 1)
26	73	(3, 8) (8, 3)	68	200	(2, 14) (10, 10) (14, 2)
27	74	(5, 7) (7, 5)	69	202	(9, 11) (11, 9)
28	80	(4, 8) (8, 4)	70	205	(3, 14) (6, 13) (13, 6) (14, 3)
29	82	(1, 9) (9, 1)	71	208	(8, 12) (12, 8)
30	85	(2, 9) (6, 7) (7, 6) (9, 2)	72	212	(4, 14) (14, 4)
31	89	(5, 8) (8, 5)	73	218	(7, 13) (13, 7)
32	90	(3, 9) (9, 3)	74	221	(5, 14) (10, 11) (11, 10) (14, 5)
33	97	(4, 9) (9, 4)	75	225	(9, 12) (12, 9)
34	98	(7, 7)	76	226	(1, 15) (15, 1)
35	100	(6, 8) (8, 6)	77	229	(2, 15) (15, 2)
36	101	(1, 10) (10, 1)	78	232	(6, 14) (14, 6)
37	104	(2, 10) (10, 2)	79	233	(8, 13) (13, 8)
38	106	(5, 9) (9, 5)	80	234	(3, 15) (15, 3)
39	109	(3, 10) (10, 3)	81	241	(4, 15) (15, 4)
40	113	(7, 8) (8, 7)	82	242	(11, 11)
41	116	(4, 10) (10, 4)	83	244	(10, 12) (12, 10)
42	117	(6, 9) (9, 6)	84	245	(7, 14) (14, 7)

4.2.3 Analysis

In all the above patterns, the following are similar to our actual experiments:

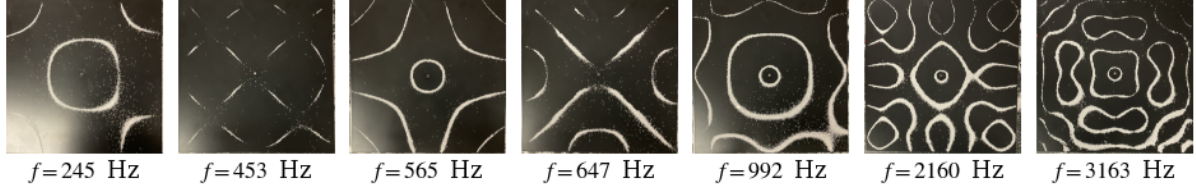


Figure 4.6: Experimental Results of the Square Plate

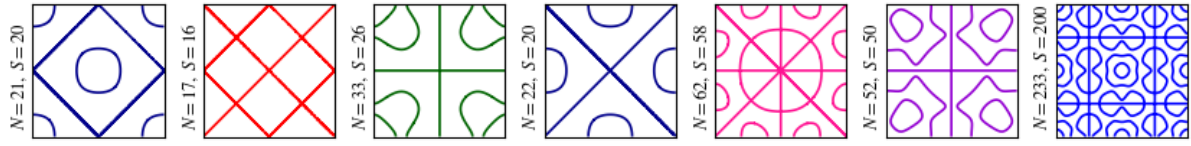


Figure 4.7: (Somewhat) Similar Patterns

Predicting the Modes. The modes and predicted wave speed of the above patterns are listed in the table below. Here, the wave speed is calculated by the formula

$$c = \frac{2Lf}{\sqrt{n^2 + m^2}} \quad (4.2.1)$$

For our experiment, the length of the plate is, $L = 24.1 \pm 0.1$ cm.

Table 4.2: Wave Speed of the Square Plate

Pattern #	Sum	Modes (n, m)	Sign	Found at Frequency	Wave Speed (m/s)
21	20	(2, 4) (4, 2)	[+, +]	245 ± 50 Hz	26.41 ± 5.39
17	16	(0, 4) (4, 0)	[+, -]	453 ± 50 Hz	54.59 ± 6.03
33	26	(1, 5) (5, 1)	[+, -]	565 ± 75 Hz	53.41 ± 7.11
22	21	(2, 4) (4, 2)	[+, -]	647 ± 75 Hz	69.73 ± 8.09
62	58	(3, 7) (7, 3)	[+, -]	934 ± 100 Hz	59.11 ± 6.33
52	50	(1, 7) (5, 5) (7, 1)	[+, +, +]	2160 ± 500 Hz	147.24 ± 34.09
223	200	(2, 14) (10, 10) (14, 2)	[+, +, +]	3163 ± 800 Hz	107.80 ± 27.27

We observed a general increasing trend in the wave speed, but some of the values do not follow the trend. The uncertainty of c is determined by

$$\sigma_c = c \sqrt{\left(\frac{\sigma_L}{L}\right)^2 + \left(\frac{\sigma_f}{f}\right)^2} \quad (4.2.2)$$

All the values are also not in each other's range of uncertainty. Therefore, we predict the wave speed indeed has an increasing trend.

4.3 Experimental and Theoretical Results for the Circular Plate

4.3.1 Experimental Results

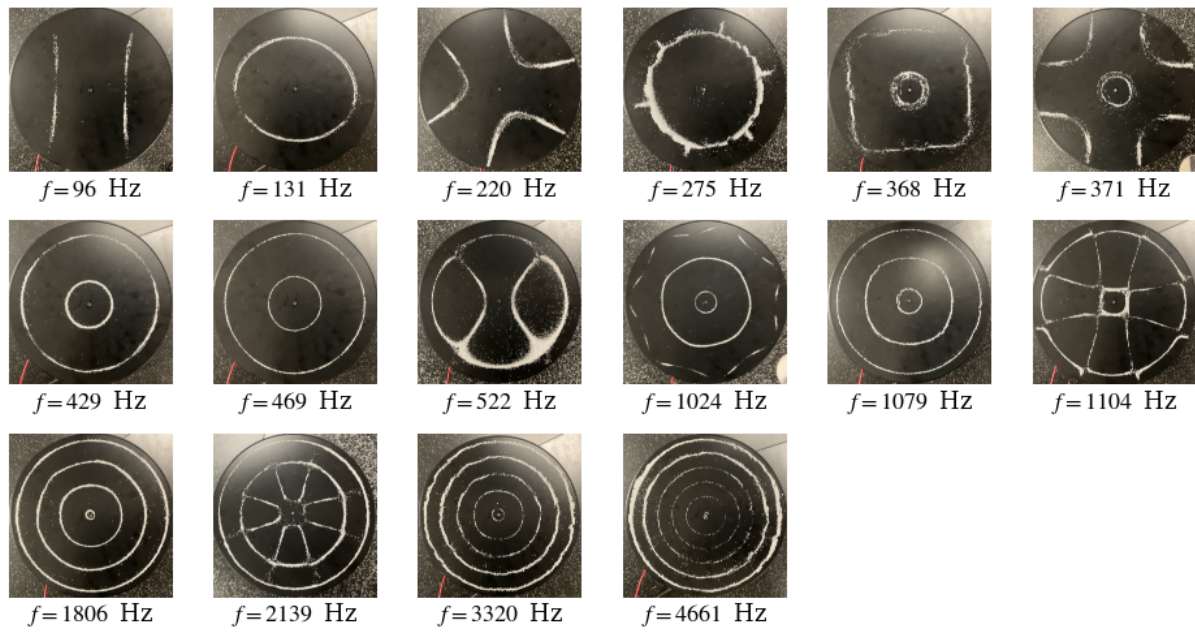


Figure 4.8: Experimental Results of the Circular Plate

4.3.2 Theoretical Results

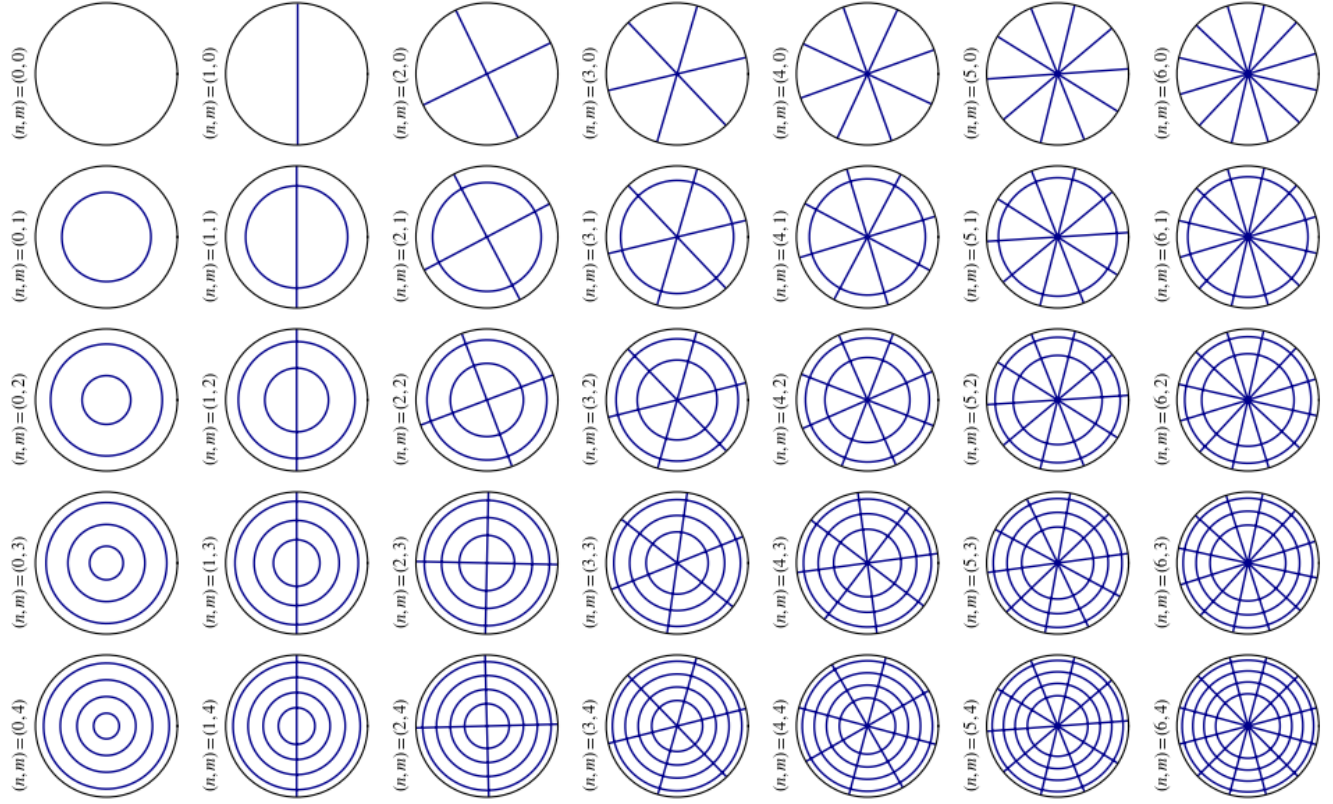


Figure 4.9: First 35 theoretical patterns of the circular plate, plotted in Python.
(From the wave equation model, might not be accurate)

4.3.3 Analysis

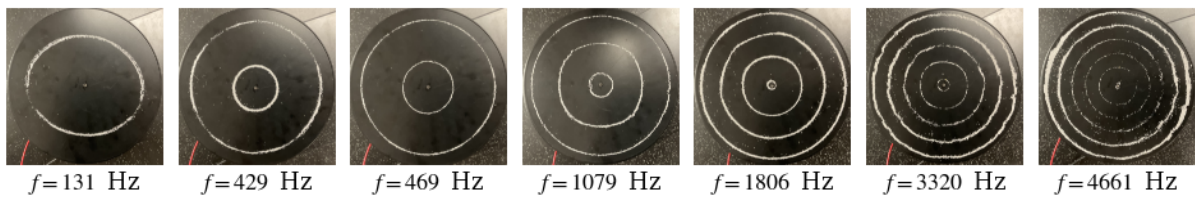


Figure 4.10: Our experimental patterns, with rings

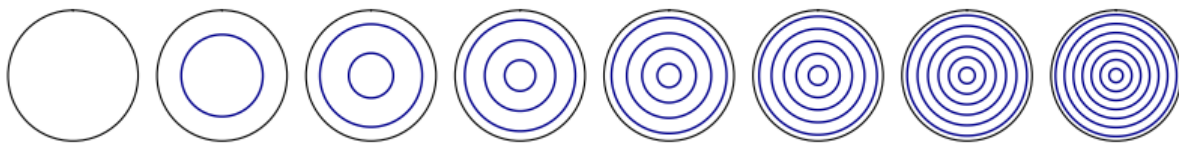


Figure 4.11: Similar Patterns, where $n = 0$, $m = 0, 1, 2, \dots, 7$

Predicting the Modes. The modes and predicted wave speed of the above patterns are listed in the table below. Here, the wave speed is calculated by the formula

$$c = \frac{2\pi fr}{z_{nm}} \quad (4.3.1)$$

For our experiment, the plate's radius is, $r = 12.1 \pm 0.1$ cm. The zeros of $J'_n(x)$ can be found using numerical algorithms. Detailed codes are provided in the appendix below.

Table 4.3: Wave Speed of the Circular Plate

Order (n)	Zero (m)	Zeroes of $J'_n(r)$	Found at Frequency	Wave Speed (m/s)
0	0	0.000000	0.000 Hz	N/A
0	1	3.831706	131 ± 50 Hz	25.885 ± 9.88
0	2	7.0155867	429 ± 75 Hz	46.298 ± 8.10
0	3	10.1734681	1079 ± 100 Hz	80.301 ± 14.05
0	4	13.3236919	1806 ± 500 Hz	102.627 ± 7.47
0	5	16.4706301	3320 ± 750 Hz	152.614 ± 34.50
0	6	19.6158585	4661 ± 800 Hz	172.184 ± 29.59

We observed a general increasing trend in the wave speed for this case. The uncertainty of c is determined by

$$\sigma_c = c \sqrt{\left(\frac{\sigma_r}{r}\right)^2 + \left(\frac{\sigma_f}{f}\right)^2} \quad (4.3.2)$$

Chapter 5

The Elastic Theory Model, the Biharmonic Wave Equation, and Chladni's Law

5.1 Theoretical Derivation

The Biharmonic Wave Equation. Although the wave equation has led to some decent approximation of a few patterns, in reality, the assumption that the displacement of the metal plate obeys the two-dimensional wave equation is almost completely false. This is because the metal plate, unlike a membrane, is not supported by tension, but by bending moment. The equation that truly describes the displacement of the plate is the Biharmonic wave equation [6], a fourth-order, time-dependent partial differential equation, described by

$$\frac{\partial^2 u}{\partial t^2} + \kappa^2 \left(\frac{\partial^4 u}{\partial x^4} + 2 \frac{\partial^4 u}{\partial x^2 y^2} + \frac{\partial^4 u}{\partial y^4} \right) = Q(x, y, t), \quad (5.1.1)$$

or, written in a more compact form:

$$u_{tt} + \kappa^2 \nabla^4 u = Q, \quad -a \leq x, y \leq a, \quad (5.1.2)$$

here,

$$\kappa^2 = \frac{Eh^2}{12\rho(1-\nu^2)}, \quad (5.1.3)$$

where p is the density, ν is Poisson's ratio, E is Young's modulus, and h is the thickness of the plate.

For a free-edge plate, the conditions that apply to this equation are the boundary conditions

$$\begin{aligned} u_{xx} + \nu u_{yy} &= 0, & u_{xxx} + (2 - \nu) u_{yyx} &= 0 \text{ along } x = \pm a \\ u_{yy} + \nu u_{xx} &= 0, & u_{yyy} + (2 - \nu) u_{yxx} &= 0 \text{ along } y = \pm a \\ u_{xy}(\pm a, \pm a, t) &= 0 \end{aligned}$$

and initial conditions:

$$u(x, y, 0) = f(x, y) \quad \text{and} \quad u_t(x, y, 0) = g(x, y)$$

Our group attempted to solve this equation in a similar way to the wave equation - by separation of variables. However, while we were on our journey to find the eigenvalues with the first two boundary conditions, we ran into an extreme difficulty: having to solve the equation

$$(p^2 + \zeta) \sin(pa) \cosh(pa) - (p^2 - \zeta) \cos(pa) \sinh(pa) = 0,$$

where

$$\zeta = (2 - \nu)Y''(y)$$

This is a very difficult task since ζ is not a number, but a function of y , so attempting to solve the eigenvalue numerically is not in the discussion. Moreover, even if we can find, and express the eigenvalues in terms of ζ , the task will be even more difficult since we now have to substitute back into the other boundary and initial conditions to solve for the exact values of the eigenvalues, making it pretty much impossible to solve for p 's. All the papers, books, and research works of various individuals that we have looked through so far have claimed that it is not possible to solve this equation analytically.

Chladni's Law. As challenging as the problem is, it does not mean that nothing meaningful can be discovered from this equation. Although the square plate is indeed extremely difficult to solve, the circular plate, on the other hand, is also difficult to solve. However, due to the symmetric nature of the circular plate, Rayleigh was able to show that

$$f = C(n + 2m)^2. \quad (5.1.4)$$

To understand the work of Rayleigh, we need to go back to one dimension. Take a 2-meter wooden ruler that we usually see in our average college classroom, and wave it. We will see that the ruler creates a standing wave. However, the equation governing the motion of the ruler is not the regular wave equation because of the reason similar to as stated above, but by the *bending beam - flexural wave equation*[7]

$$\frac{\partial^2 u}{\partial t^2} + c_L^2 K^2 \frac{\partial^4 u}{\partial x^4} = 0. \quad (5.1.5)$$

Here, c_L is the longitudinal wave speed,

$$c_L = \sqrt{\frac{E}{\rho}}, \quad (5.1.6)$$

where E is Young's modulus and ρ is density. This is a bit different in two dimensions since there are lateral expansions in 2D. Authors Rossing and Fletcher [8] mentioned in their work *Two-Dimensional Systems: Membranes and Plates*[9], that the correct equation for c_L for a plate is

$$c_L = \sqrt{\frac{E}{\rho(1 - \nu^2)}}, \quad (5.1.7)$$

where ν is the ratio of lateral contraction to longitudinal elongation (also known as Poisson's ratio).

Rayleigh's Derivation of the Formula. Going back to the biharmonic equation above. Since we know that the forcing function should not affect the general shape of the patterns, we can assume that $Q = 0$ and rewrite it as

$$\nabla^4 u - \frac{12\rho(1 - \nu^2)}{Eh^2} u_{tt} = 0. \quad (5.1.8)$$

Apply separation of variables once again, but this time, only separate the time variable, $u(x, y, t) = U(x, y)e^{i\omega t}$. Thus, $u_{tt} = \omega^2 U(x, y)e^{i\omega t}$. Substitute in, and simplify, we obtain

$$\nabla^4 U - \frac{12\rho(1-\nu^2)\omega^2}{Eh^2} U = \nabla^4 U - k^4 U = 0. \quad (5.1.9)$$

Notice that here, we define k as

$$k^2 = \frac{\sqrt{12}\omega}{h} \sqrt{\frac{\rho(1-\nu^2)}{E}} = \frac{\sqrt{12}\omega}{hc_L}. \quad (5.1.10)$$

By dimensional analysis, it is not too hard to see that this k is the familiar “wave number” that we know of. Therefore,

$$f = \frac{\omega}{2\pi} = \frac{1}{2\pi\sqrt{12}} c_L h k^2. \quad (5.1.11)$$

As stated by Rayleigh, Kirchhoff previously proved that [2]

$$\tan\left(ka - \frac{1}{2}n\pi\right) = \frac{\frac{A_2}{8ka} + \frac{A_3}{(8ka)^2} - \frac{A_4}{(8ka)^3} + \dots}{A_1 + \frac{A_2}{8ka} + \frac{A_4}{(8ka)^3} + \dots}, \quad (5.1.12)$$

where

$$\begin{aligned} A_1 &= \gamma = (1-\nu)^{-1} \\ A_2 &= \gamma(1-4n^2) - 8 \\ A_3 &= \gamma(1-4n^2)(9-4n^2) + 48(1+4n^2) \\ A_4 &= -\frac{\gamma}{3}[(1-4n^2)(9-4n^2)(13-4n^2)] + 8(9+136n^2+80n^4) \end{aligned} \quad (5.1.13)$$

Notice that the numerator approaches zero faster than the denominator as $k \rightarrow \infty$. Since f and k^2 are proportional, as $f \rightarrow \infty$, $k \rightarrow \infty$, and hence

$$\tan\left(ka - \frac{1}{2}n\pi\right) = 0 \quad \text{as } k \rightarrow \infty. \quad (5.1.14)$$

Solving for k , we obtain

$$k = \frac{\pi}{2a}(n+2m) = \frac{\pi}{d}(n+2m). \quad (5.1.15)$$

Substitute this back into the frequency equation above, we obtain

$$f = \frac{1}{\pi 4\sqrt{3}} hc_L k^2 = \frac{h\pi}{4\sqrt{3}d^2} \sqrt{\frac{E}{\rho(1-\nu^2)}} \cdot (n+2m)^2, \quad (5.1.16)$$

where E is Young’s modulus, ρ is density, ν is the ratio of lateral contraction to longitudinal elongation (also known as Poisson’s ratio), h is the thickness, and d is the diameter of the plate.

Effective Wave Speed. Authors Rossing and Fletchers also mentioned in *Principles of Vibration and Sound* that the waves in the bending plate are “dispersive,” and their speed depends on the frequency,

$$c(f) = \frac{\omega}{k} = \sqrt{\frac{2\pi hc_L}{4\sqrt{3}}} f = \sqrt{2\pi h} \sqrt{\frac{E}{12\rho(1-\nu^2)}} \cdot f^{1/2}. \quad (5.1.17)$$

This might explain why our wave speed has an increasing trend in the last section.

5.2 Data Analysis

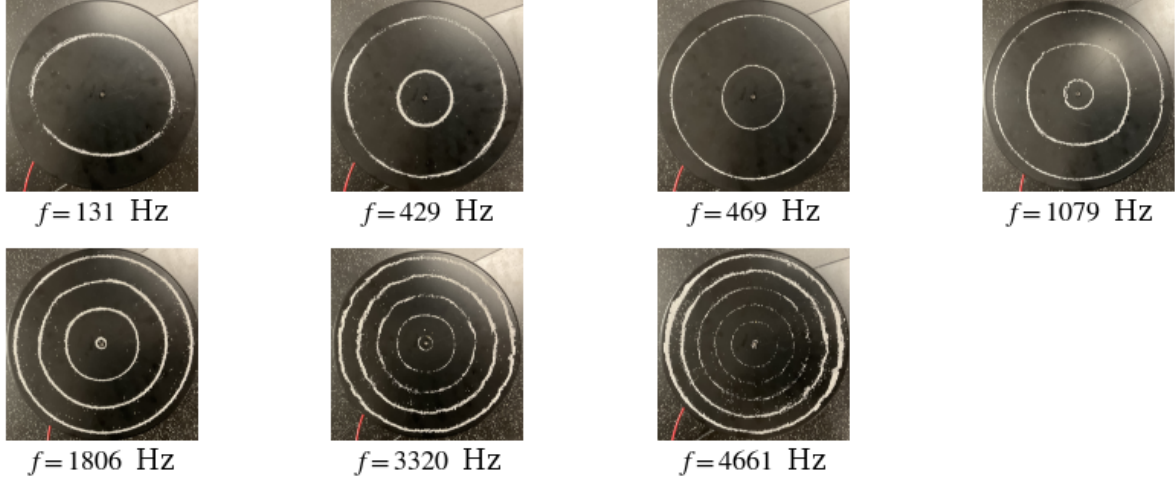


Figure 5.1: Patterns with Rings in Circular Plate

By counting the number of rings on each pattern listed above, we can make a table as below

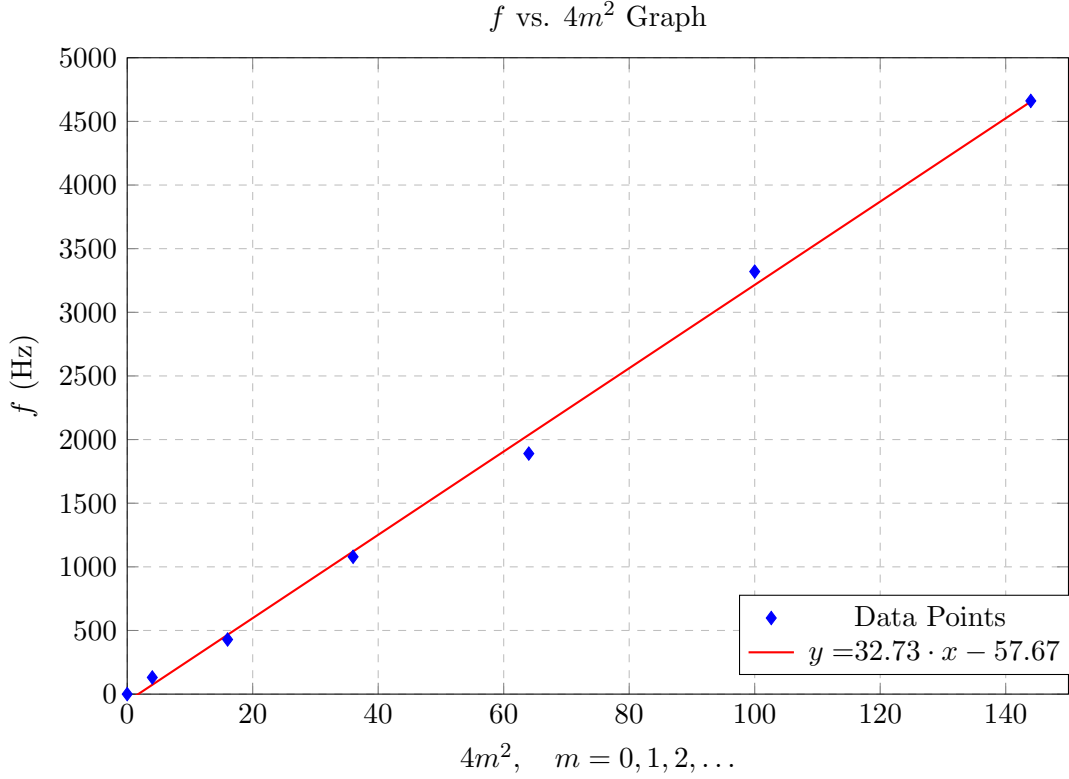
Table 5.1: f vs. $4n^2$ table

m	$4m^2$	f (Hz)
0	0	0
1	4	131
2	16	429
3	36	1079
4	64	1806
5	100	3320
6	144	4661

Since there are no diameter lines, $n = 0$. The equation for f becomes

$$f = \frac{1}{\pi 4\sqrt{3}} hc_L k^2 = \frac{h\pi}{4\sqrt{3}d^2} \sqrt{\frac{E}{\rho(1-\nu^2)}} \cdot (2m)^2, \quad (5.2.1)$$

This implies that f and $(2m)^2$ have a linear relationship. Therefore, we plotted our data below to test this theory.



Note* by taking this data set to excel, we were able to obtain an R^2 value of 0.998, which is an almost perfect correlation!

Comparison with the True Value. The plate is made of Aluminum, which has the following properties: $E = 68$ GPa, $\rho = 2710$ kg/m³, $\nu = 0.33$, $h = 0.8 \pm 0.3$ mm, $d = 0.241 \pm 0.001$ m. Therefore, the coefficient C is determined by

$$C = \frac{1}{\pi 4\sqrt{3}} hc_L = \frac{h\pi}{d^2} \sqrt{\frac{E}{12\rho(1-\nu^2)}} = \kappa\pi \frac{h}{d^2} = 33.1430, \quad (5.2.2)$$

which is very close to our linear fit. The uncertainty of C can be calculated by

$$\sigma_C = \sqrt{\left(\frac{\partial C}{\partial h}\sigma_h\right)^2 + \left(\frac{\partial C}{\partial d}\sigma_d\right)^2} = C \sqrt{\left(\frac{\sigma_h}{h}\right)^2 + \left(\frac{2h\sigma_d}{d}\right)^2} = 12.43. \quad (5.2.3)$$

The coefficient C lies within our uncertainty range, which once again verifies the validity of Chladni's law.

Chapter 6

Conclusion

In performing this complex experiment, we were able to attain very noticeable patterns in both the square and circular plates. However, we failed to prove our hypothesis correct. That is, we failed to show that the wave speed remains constant over different frequencies. As a matter of fact, we observed the exact opposite - a linear relationship in the circular plate and a general increasing trend in the square plate.

Our failures can be mainly attributed to the equipment we have access to. For example, the plates we used had very small, (but definitely significant) imperfections all over the surface of the plate. This could include stuff like paint, dirt, and manufacturing impurities within the plate. These almost microscopic inclusions play a *huge* role in the accuracy of the patterns we receive.

Another attribute of our error is the leveling of the table. Although we chose the most level table, there was still an ever-so-slight incline in the experiment, which matters greatly when dealing with the light sand. Additionally, the oscillator was not stable and in line with the plates, so when the oscillator vibrated, the plates would “shake” out of control with respect to the scale of the lab.

However, our true flaw within this experiment comes from our very inaccurate (albeit the best we have) wave equation. The actual equation that describes the plate is the *Biharmonic wave equation*

$$\frac{\partial^2 u}{\partial t^2} + k^2 \left(\frac{\partial^4 u}{\partial x^4} + 2 \frac{\partial^4 u}{\partial x^2 \partial y^2} + \frac{\partial^4 u}{\partial y^4} \right) = Q, \quad \text{or} \quad u_{tt} + k^2 \nabla^4 u = Q, \quad -a \leq x, y \leq a$$

This equation is a fourth-order partial differential equation, and therefore extremely difficult to solve even with simple boundary conditions, but with the given set of boundary-initial conditions, we found out that it was truly impossible to solve since it requires us to solve for multiple sets of undiscovered, non-elementary eigenvalues.

The uncertainty in this lab was almost stymied by the intimidating equations that describe the plate. However, by taking our more elementary and less intimidating approach of finding an R^2 of the set of data points in Chaldni’s Law for effective wave speed in Sec. (5.1), we were able to gauge how valid our data was. Surprisingly, our data was extremely good when looking at our observed linear case. Moreover, we were able to get an interval in which our coefficient C was valid over. We found our theoretical to be 33.1430 ± 12.43 , while our experimental sat at 33.73, which is surprisingly close! Our uncertainty was very large in C since Young’s modulus E is *very* large.

For the square plate, we were unable to find a relevant equation relating to the (general) increasing trend in the wave speed of the plate. It is important to note that the trend is not as noticeable in the square plate because the uncertainty in the frequency in the square plate was *much much* larger than the uncertainty in the circular plate for some unknown reason. In the larger f values, we saw that resonance occurred in intervals of ± 800 Hz for some f values! We are left to simply observe that the wave speed does not depend on the frequency in both cases. However, we were only able to find a relationship to the circular plate. Taking into account the uncertainty in the square plate comfortably accounts for the deviation in the upward trend in the wave speed.

Although we were limited by our own knowledge and could not proceed further due to time constraints, a recent paper from 2020, titled “Stable and Accurate Numerical Methods for Generalized Kirchhoff-Love Plates,” [10] by authors Nguyen, Li, and Ji, accurately modeled the patterns on Chladni plates. We found that the plates in their paper have the same dimensions as ours, and the patterns on the plates are also identical, appearing at frequencies very close to ours. The paper used the full Biharmonic Equation

$$\rho h \frac{\partial^2 w}{\partial t^2} = -D \nabla^4 w + T \nabla^2 w - K_0 w - K_1 \frac{\partial w}{\partial t} + T_1 \nabla^2 \frac{\partial w}{\partial t} + F(\mathbf{x}, t), \quad (6.0.1)$$

Here, ρ is the density, K_0 is the linear stiffness coefficient, representing the linear storing force, T is the tension coefficient, K_1 is the linear damping term, T_1 is the visco-elastic damping coefficient, and $F(\mathbf{x}, t)$ is the forcing function. Moreover, D is defined as

$$D = \frac{Eh^3}{12(1-\nu^2)}, \quad (6.0.2)$$

which includes the flexural rigidity constant ν , E is young’s modulus, and h is the thickness of the plate. This finding was truly fascinating to us, as such a simple object such as a metal plate can have such a complicated mathematical model. Though the biharmonic equation is not analytically solvable for any plate, they were able to find the patterns using numerical approximation algorithms. It is interesting to note that the constant D satisfies the unknown equation, and its similarities to the constant C for the circular plate are prevalent.

Though we failed to prove the consistency of the wave speed in the harmonic plates, our experiment reversed our expectations regarding the wave nature of the oscillating plates. As we began to notice an almost certain discontinuity in the wave speed of our plates, we searched through various books and research papers for possible explanations. Chaldni’s law for a circular plate caught our eye, and after finding that our data closely matched that model, we applied the equations to our own and found an almost perfect correlation ($R^2 = 0.998!$). We were able to definitely conclude that the wave speed in fact *does not* remains constant and disperses outwards depending on the frequency, and other material-dependant constants, including the geometry of the plate. Although this validated our circular plate’s linear wave speed, our square plate is unfortunately left to be desired, as we were unable to find an equation that could account for the similar trend in the wave speed (Though there is *absolutely* an increasing trend). Our endeavors within this realm of physics propel us into bigger and more interesting ideas. We have found and mathematically revealed the presence of these resonance states at the 1st and 2nd dimensions. However, a mathematical model describing the true model of these extravagant plates has yet to be discovered, and so, as of now, we remain humbled by the beautiful nature of physics. Thus, curiosity drives, and physics prevails.

Appendices

Appendix A

Mathematical Preliminaries

A.1 Regular Sturm-Liouville Theory

Definition A.1.1. Consider the Sturm-Liouville problem

$$\frac{1}{w(x)}[(p(x)y')' + q(x)y] + \lambda y = 0, \quad a < x < b, \quad (\text{A.1.1})$$

$$\alpha_1 y(a) + \alpha_2 y'(a) = 0 \quad (\text{A.1.2})$$

$$\beta_1 y(b) + \beta_2 y'(b) = 0 \quad (\text{A.1.3})$$

If each of the following conditions is satisfied:

1. $p, q, w, p' \in C[a, b]$,
2. $p(x)$ and $q(x) > 0$, for all $x \in [a, b]$,
3. $\alpha_1^2 + \alpha_2^2 \neq 0$ and $\beta_1^2 + \beta_2^2 \neq 0$,

then we call the Sturm-Liouville problem above regular.

Theorem A.1.1. [3] Let

$$\frac{1}{w(x)}[(p(x)y')' + q(x)y] + \lambda y = 0, \quad a < x < b, \quad (\text{A.1.4})$$

$$\alpha_1 y(a) + \alpha_2 y'(a) = 0 \quad (\text{A.1.5})$$

$$\beta_1 y(b) + \beta_2 y'(b) = 0 \quad (\text{A.1.6})$$

be a regular Sturm-Liouville problem. Then, the following holds true:

- (a) All eigenvalues of this problem are real and can be arranged into an increasing sequence

$$\lambda_1 < \lambda_2 < \dots < \lambda_n < \lambda_{n+1} < \dots, \quad n \rightarrow \infty$$

- (b) The eigenfunction sequence $\{y(x)\}_{n=1}^{\infty}$ forms a complete orthogonal family on the interval (a, b) with respect to the weight function $w(x)$. Meaning that, if λ_n and λ_m are two distinct eigenvalues with corresponding eigenfunctions $y_n(x)$ and $y_m(x)$, then their weighted inner product is zero; i.e.

$$\langle y_n, y_m \rangle_w = \int_a^b y_n(x)y_m(x)w(x)dx = 0, \quad n \neq m$$

- (c) Each eigenfunction $y_n(x)$ that correspond to an eigenvalue λ_n is unique up to a constant multiple.
- (d) Let $L_w^2[a, b]$ denotes the weighted L^2 space, defined by

$$L_w^2[a, b] = \left\{ f : [a, b] \rightarrow \mathbb{R} \mid \int_a^b |f(x)|^2 w(x) dx < \infty \right\}.$$

If $f \in L_w^2[a, b]$ is expanded as an infinite series of orthogonal functions

$$f(x) = \sum_{n=1}^{\infty} c_n y_n(x), \quad a < x < b,$$

then the coefficients c_n are determined by

$$c_n = \frac{\langle f, y_n \rangle_w}{\langle y_n, y_n \rangle_w} = \frac{\int_a^b f(x) y_n(x) y_m(x) w(x) dx}{\int_a^b y_n^2(x) w(x) dx}.$$

A.2 Singular Sturm-Liouville Theory

Definition A.2.1. Consider the Sturm-Liouville problem

$$\frac{1}{w(x)} [(p(x)y')' + q(x)y] + \lambda y = 0, \quad a < x < b, \quad (\text{A.2.1})$$

$$\alpha_1 y(a) + \alpha_2 y'(a) = 0 \quad (\text{A.2.2})$$

$$\beta_1 y(b) + \beta_2 y'(b) = 0 \quad (\text{A.2.3})$$

If each of the following conditions is satisfied:

1. $p, q, w, p' \in C[a, b]$,
2. $p(x)$ and $q(x) > 0$, for all $x \in [a, b]$,

and at least one of the conditions below holds true:

1. $a = -\infty$ or $b = +\infty$,
2. $p(x)$ or $w(x)$ is zero at an endpoint,
3. p, q , or w becomes infinite at an endpoint.

then we call the Sturm-Liouville problem above a singular Sturm-Liouville problem.

As seen in the circular plate, the method of separation of variables may oftentimes lead to singular Sturm-Liouville problems. To make sense of the boundary condition, the boundary conditions of the PDE can be modified based on the actual physical condition of the DE. The key here is to keep the Sturm-Liouville operator \mathcal{S} , defined as

$$\mathcal{S}y := \frac{1}{w(x)} [(p(x)y')' + q(x)y]$$

symmetric; that is, $\langle u, \mathcal{S}v \rangle_w = \langle \mathcal{S}u, v \rangle_w$. For more information, consider consulting *Introduction to Applied Partial Differential Equation* by John M. Davis.

Appendix B

Codes in Python

B.1 Starting out with Python

The majority of plots in this project are plotted in Python. Python is a high-level programming language used extensively in the STEM fields due to its flexibility and clear code syntax. One can download Python at python.org/downloads/.

After installing the language, we need an IDE like Jetbrains PyCharm, or a text editor like Visual Studio code to write our code on. There are plenty of tutorials online on how to set this up.

After setting everything up, we now move to the miracle of Python - the library management system. Unlike other languages like C++, where you have to link the libraries manually, modern Python has a built-in library/package management system. To install the necessary packages needed for the program, simply open the command prompt, and enter the following command

```
-m pip install [your_package_here]
```

For this specific project, we need *matplotlib* to plot on a coordinate system, *numpy* for the mathematical functions, *itertools* for signs alternation tool, *scipy* for integration and special functions, so just paste the following commands one at a time into the command prompt:

```
-m pip install matplotlib  
-m pip install numpy  
-m pip install itertools  
-m pip install scipy
```

B.2 Code for the Square Wave Equation Plot

```
1 import matplotlib.pyplot as plt  
2 import numpy as np  
3 import itertools  
4  
5 # Settings here  
6 title = True  
7 font_title = 9.2      # Title font size  
8 color_plots = True    # All black or color plots  
9 thickness = 1.2       # Plot line thickness  
10 start = 1            # Start at pattern #
```

```

11 end = 72           # End at pattern #
12
13 # Range and step size
14 delta = 0.005
15 xrange = np.arange(-1.0, 1.0, delta)
16 yrange = np.arange(-1.0, 1.0, delta)
17 x, y = np.meshgrid(xrange, yrange)
18
19 # Define the basis function
20 def X(x, n):
21     return np.mod(n + 1, 2) * np.cos(n * np.pi * x / 2.0)
22     + np.mod(n, 2) * np.sin(n * np.pi * x / 2.0)
23
24 # Sign combination generator
25 def generate_sign_combinations(pairs):
26     sign_combinations = list(itertools.product([1, -1], repeat=(len(pairs) - 1)))
27     return [[1] + list(comb) for comb in sign_combinations] # Keep the first sign positive
28
29 # The wave function with contour cut z = 0
30 def u(x, y, pairs, signs):
31     equation = np.zeros_like(x) # Return an array of 0's with the same type
32     for (n, m), sign in zip(pairs, signs):
33         equation += sign * X(x, n) * X(y, m)
34     return equation
35
36 # Searching combinations of sum of squares
37 def find_pairs(number):
38     return [(n, m) for n in range(0, int(np.sqrt(number)) + 1)
39             for m in range(0, int(np.sqrt(number)) + 1) if n**2 + m**2 == number]
40
41 # Check if a given number has sums of squares pairs
42 def exist_sos(number):
43     return any(n**2 + m**2 == number for n in range(0, int(np.sqrt(number)) + 1)
44                         for m in range(0, int(np.sqrt(number)) + 1))
45
46
47 plt.rcParams['mathtext.fontset'] = 'stix'
48 plt.rcParams['font.family'] = 'serif'
49
50 # Plot the sum of squares patterns from start_index to end_index (1-based indexing)
51 def plot_sum_of_squares(start_index, end_index):
52     total_plots = end_index - start_index + 1
53
54     # Error messages
55     if end_index <= start_index:
56         print("Error: End_index must be greater than start_index.\n")
57         return
58     if total_plots > 100:
59         print("Error: Cannot plot more than 100 plots at a time.\n")
60         return
61
62     equations = []
63     descriptions = []
64     sums_of_squares = []
65
66     # Iterating over all possible combinations
67     k = 0
68     found_plots = 0

```

```

69     while len(equations) < total_plots:
70         if exist_sos(k):
71             pairs = find_pairs(k)
72             non_zero_pairs = pairs[1:-1]
73             sign_combinations = generate_sign_combinations(pairs)
74             for signs in sign_combinations:
75                 found_plots += 1
76                 if start_index <= found_plots <= end_index:
77                     equations.append((pairs, signs, u(x, y, pairs, signs)))
78                     descriptions.append(f"{pairs} {signs}")
79                     sums_of_squares.append(k)
80                 if found_plots >= end_index:
81                     break
82             if non_zero_pairs:
83                 sign_combinations_0 = generate_sign_combinations(non_zero_pairs)
84                 for signs in sign_combinations_0:
85                     found_plots += 1
86                     if start_index <= found_plots <= end_index:
87                         equations.append((non_zero_pairs, signs, u(x, y, non_zero_pairs, signs)))
88                         descriptions.append(f"{non_zero_pairs} {signs}")
89                         sums_of_squares.append(k)
90                     if found_plots >= end_index:
91                         break
92                 if found_plots >= end_index:
93                     break
94             k += 1
95
96     # Fixed number of columns
97     ncols = 9
98     # Calculate the number of rows (// = Floor division)
99     nrows = (total_plots + ncols - 1) // ncols
100
101    # Define fig and axis
102    fig, axs = plt.subplots(nrows, ncols, figsize=(1.2 * ncols, 4 * nrows))
103
104    # Colors
105    colors = ['darkblue', 'red', 'darkgreen', 'deeppink', 'darkviolet', 'blue', 'darkgoldenrod',
106              'teal', 'darkred', 'darkcyan']
107    pair_color_mapping = {}
108    color_index = 0
109
110    # Plotting
111    for i in range(total_plots):
112        # Print all pairs and signs to the console
113        print(f"N = {start + i} | S = {sums_of_squares[i]}: {descriptions[i]}")
114
115        # pairs = equations[i][0], signs = equations[i][1], equation = equations[i][2]
116        pairs, signs, equation = equations[i]
117        pairs_tuple = tuple(pairs)
118        if pairs_tuple not in pair_color_mapping:
119            pair_color_mapping[pairs_tuple] = colors[color_index % len(colors)]
120            color_index += 1
121
122        mode_color = pair_color_mapping[pairs_tuple] if color_plots else 'black'
123        row, col = divmod(i, ncols)
124        plot_title = rf"$N = {start + i},\backslash; S = {sums_of_squares[i]}$"
125
126        ax = axs[row, col] if nrows > 1 else axs[col]

```

```

127     ax.contour(x, y, equation, levels=[0], colors=mode_color, linewidths=thickness)
128
129     if title:
130         ax.set_title(plot_title, fontsize=font_title, ha='center', rotation='vertical',
131                     x=-0.1,y=0)
132     ax.grid(True)
133     ax.set_aspect('equal')
134     ax.set_xticks([])
135     ax.set_yticks([])
136
137     plt.tight_layout()
138     fig.subplots_adjust(hspace=0.2, wspace=0.1)
139     plt.show()
140
141 # Plotting the Chladni's pattern
142 plot_sum_of_squares(start, end)

```

B.3 Code for the Circular Wave Equation Plot

```

1 import matplotlib.pyplot as plt
2 import numpy as np
3 import scipy.integrate as integrate
4 from scipy.special import jn, jnp_zeros
5
6 a = 1.0                      # Radius of the plate
7 thickness = 1                  # Line thickness
8 color = 'darkblue'             # Color
9 title = True                   # Title?
10 columns = 7
11 rows = 5
12
13 # Function to get the m-th zero of the derivative of the Bessel function of order n
14 def bessel_derivative_zero(n, m):
15     if n == 0: #Redefine the first zero of J_0 prime to be 0
16         zeros = list(jnp_zeros(n, m + 1))
17         zeros.insert(0, 0)
18         return zeros[m]
19     else:
20         return jnp_zeros(n, m + 1)[-1] # Get the m-th zero, treating first zero as the 0th zero
21
22
23 # Initial function f(r, theta)
24 def f(r, theta):
25     return r * np.cos(theta)
26
27 # Define the double integrals for coefficients a_nm and b_nm
28 def a_nm(n, m, a):
29     z_nm = bessel_derivative_zero(n, m)
30     numerator = integrate dblquad(lambda theta, r: jn(n, z_nm * r * 1.0/a) * np.cos(n * theta) *
31                                     f(r, theta) * r, 0, a, lambda r: 0, lambda r: 2 * np.pi)[0]
32     denominator = integrate quad(lambda r: jn(n, z_nm * r * 1.0/a) ** 2 * r, 0, a)[0]
33     return numerator / (2 * np.pi * denominator)
34
35 def b_nm(n, m, a):
36     z_nm = bessel_derivative_zero(n, m)
37     numerator = integrate dblquad(lambda theta, r: jn(n, z_nm * r * 1.0/a) * np.sin(n * theta) *

```

```

38             f(r, theta) * r, 0, a, lambda r: 0, lambda r: 2 * np.pi)[0]
39     denominator = integrate.quad(lambda r: jn(n, z_nm * r * 1.0/a) ** 2 * r, 0, a)[0]
40     return numerator / (2 * np.pi * denominator)
41
42 # Define the function  $J_n(z_{nm} * r / a) * (a_{nm} * \cos(n\theta) + b_{nm} * \sin(n\theta))$ 
43 def u(n, m, r, theta, a):
44     z_nm = bessel_derivative_zero(n, m)
45     A_nm = a_nm(n, m, a)
46     B_nm = b_nm(n, m, a)
47     return jn(n, z_nm * r * 1.0/a) * (A_nm * np.cos(n * theta) + B_nm * np.sin(n * theta))
48
49 plt.rcParams['mathtext.fontset'] = 'stix'
50 plt.rcParams['font.family'] = 'serif'
51
52 # Plotting function in polar coordinates
53 def plot_polar_contour(n_max, m_max, a, resolution=100):
54     r = np.linspace(0, a, resolution)
55     theta = np.linspace(0, 2 * np.pi, resolution)
56     R, Theta = np.meshgrid(r, theta)
57
58     if n_max < 1 or m_max < 1:
59         print("Columns or lines cannot be less than 1\n")
60         return
61
62 # Define fig and axis
63 fig, axs = plt.subplots(m_max, n_max, figsize=(1.4* n_max, 1.2 * m_max), subplot_kw=
64     {'projection': 'polar'})
65
66 for m in range(m_max):
67     for n in range(n_max):
68         Z = u(n, m, R, Theta, a)
69         ax = axs[m, n] if m_max > 1 else axs[n]
70         ax.contour(Theta, R, Z, levels=[0], colors=color, linewidths=thickness)
71         ax.set_xticks([])
72         ax.set_yticks([])
73         ax.grid(False)
74
75         plot_title = rf"${(n,m)} = {n, m}$"
76         if title:
77             ax.set_title(plot_title, fontsize = 9, ha='center', rotation='vertical',
78                         x=-0.1, y=0)
79
80     plt.tight_layout()
81     plt.show()
82
83 plot_polar_contour(columns, rows, a)
84

```

B.4 Finding Zeros of the Derivative of the Bessel Function

```

1 from scipy.special import jnp_zeros
2
3 n = 0    # Order of the Bessel function
4 m = 7    # Zero number
5
6 def bessel_derivative_zero(n, m):
7     if n == 0:

```

```
8     zeros = list(jnp_zeros(n, m + 1))
9     zeros.insert(0, 0)
10    return zeros[m]
11 else:
12     return jnp_zeros(n, m + 1)[-1] # Get the m-th zero, treating first zero as the 0th zero
13
14
15 for i in range (m):
16     zero = bessel_derivative_zero(n, i)
17     print(round(zero, 7) )
```

Bibliography

- [1] Linqi. Shao. Modeling a square vibrating plate. *University of Waterloo*, pages 1–58, 2018.
- [2] Lord Rayleigh. *Vibration of Plates*, pages 352–361. Princeton University Press, New York, NY, 1894.
- [3] John M. Davis. *Introduction to Applied Partial Differential Equation*. W. H. Freeman, New York City, 1st edition, 2012.
- [4] Richard. Haberman. *Applied Partial Differential Equations with Fourier Series and Boundary Value Problems*. Pearson, New York City, 5th edition, 2018.
- [5] Dong Du Le. Physics 4c project. https://github.com/Continuum3416/Physics_4C_Project, 2024.
- [6] Rudolph. Szilard. *Theories and Applications of Plates Analysis*. John Wiley and Sons, Inc., 111 River Street Hoboken, NJ 07030-5774, 2004.
- [7] Dispersion of flexural waves. <https://www.acs.psu.edu/drussell/Demos/Dispersion/Flexural.html>, 2004. Accessed: 2024-05-26.
- [8] Thomas D. Rossing and Neville H. Fletcher. *Principles of Vibration and Sound*. Springer, New York City, 15th edition, 2004.
- [9] Thomas D. Rossing and Neville H. Fletcher. *Two-Dimensional Systems: Membranes and Plates*, pages 65–94. Springer New York, New York, NY, 2004.
- [10] Dzmitry Bahdanau, Kyunghyun Cho, and Yoshua Bengio. Stable and accurate numerical methods for generalized kirchhoff-love plates, 2020. Accessed: 2024-05-26.